DEPARTMENT OF PRODUCTION ENGINEERING

Programme B.Tech

Semester-5th

Course Title: THEORY OF METAL CUTTING

COURSE CODE: BPE 301

MODULE-1

Geometry of single point turning tools

Both material and geometry of the cutting tools play very important roles on their performances in achieving effectiveness, efficiency and overall economy of machining. Cutting tools may be classified according to the number of major cutting edges (points) involved as follows:

- Single point: e.g., turning tools, shaping, planning and slotting tools and boring tools
- Double (two) point: e.g., drills
- Multipoint (more than two): e.g., milling cutters, broaching tools, hobs, gear shaping cutters etc.

1. Concept of rake and clearance angles of cutting tools.

The word tool geometry is basically referred to some specific angles or slope of the salient faces and edges of the tools at their cutting point. Rake angle and clearance angle are the most significant for all the cutting tools.

The concept of rake angle and clearance angle will be clear from some simple operations shown in Fig. 1.1

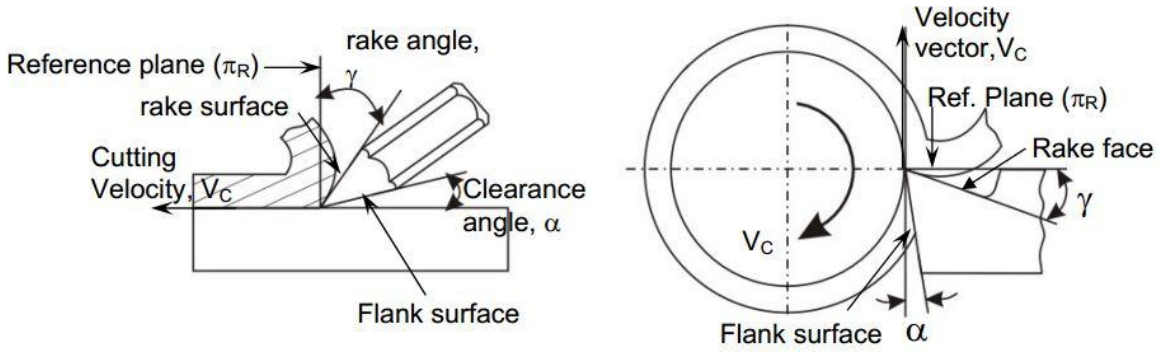

Fig. 1.1 Rake and clearance angles of cutting tools.

- Rake angle (γ): Angle of inclination of rake surface from reference plane
- clearance angle (α): Angle of inclination of clearance or flank surface from the finished surface
- Rake angle is provided for ease of chip flow and overall machining. Rake angle may be positive, or negative or even zero as shown in Fig. 1.2

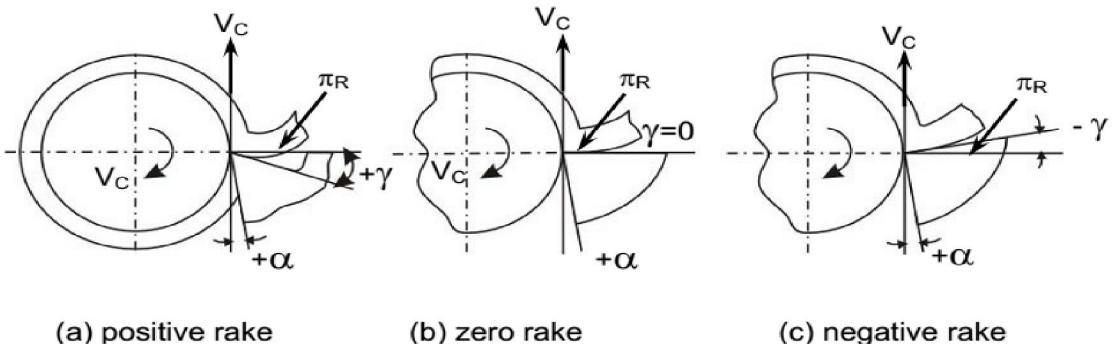

Fig. 1.2Three possible types of rake angles

Relative advantages of such rake angles are:

- Positive rake – helps reduce cutting force and thus cutting power requirement.
- Negative rake – to increase edge-strength and life of the tool
- Zero rake – to simplify design and manufacture of the form tools.

Clearance angle is essentially provided to avoid rubbing of the tool (flank) with the machined surface which causes loss of energy and damages of both the tool and the job surface. Hence, clearance angle is a must and must be positive (3^o~ 15^o) depending upon tool-work materials and type of the machining operations like turning, drilling, boring etc.

Systems of description of tool geometry

- Tool-in-Hand System – where only the salient features of the cutting tool point are identified or visualized as shown in Fig. 1.3. There is no quantitative information, i.e., value of the angles.

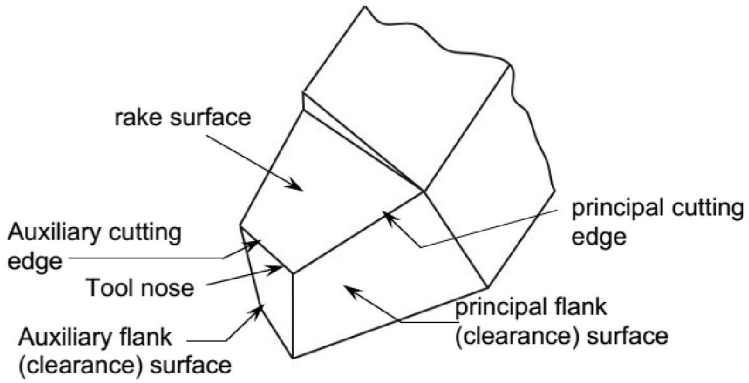

Fig. 1.3 Basic features of single point tool (turning) in Tool-in-hand system

- Machine Reference System – ASA system
- Tool Reference Systems
    - Orthogonal Rake System – ORS
    - Normal Rake System – NRS
- Work Reference System – WRS

(iii) Demonstration (expression) of tool geometry in:

Machine Reference System

This system is also called ASA system; ASA stands for American Standards Association. Geometry of a cutting tool refers mainly to its several angles or slope of its salient working surfaces and cutting edges. Those angles are expressed w.r.t. some planes of reference. In Machine Reference System (ASA), the three planes of reference and the coordinates are chosen based on the configuration and axes of the machine tool concerned. The planes and axes used for expressing tool geometry in ASA system for turning operation are shown in Fig. 1.4

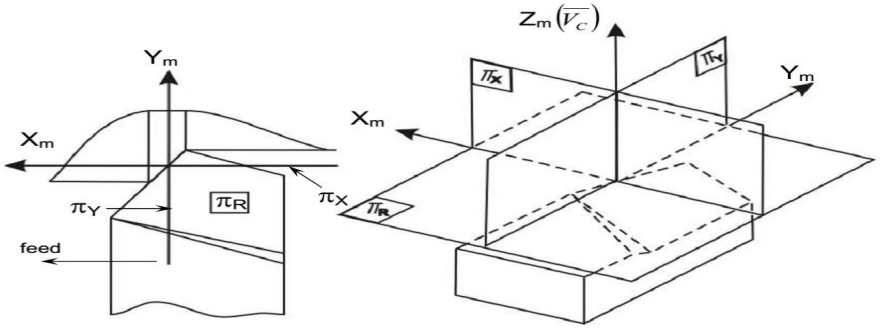

Fig. 1.4 Planes and axes of reference in ASA system

The planes of reference and the coordinates used in ASA system for tool geometry are: π_R- π_X- π_Y and X_m– Y_m- Z_m

Where,

π_R= Reference plane; plane perpendicular to the velocity vector (shown in Fig. 1.4)

π_X = Machine longitudinal plane; plane perpendicular to π_R and taken in the direction of assumed longitudinal feed

π_Y= Machine Transverse plane; plane perpendicular to both π_R and π_X [This plane is taken in the direction of assumed cross feed]

The axes X_m, Y_m and Z_m are in the direction of longitudinal feed cross feed and cutting velocity (vector) respectively. The main geometrical features and angles of single point tools in ASA systems and their definitions will be clear from Fig. 1.5

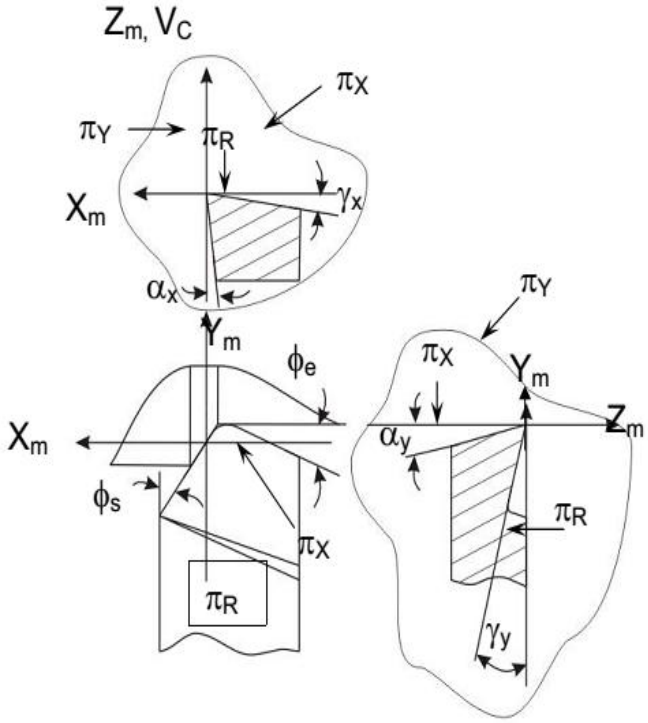

Fig. 1.5 Tool angles in ASA system

Definition of:

• Rake angles: [Fig. 1.5] in ASA system

γ_x= side (axial rake: angle of inclination of the rake surface from the reference plane (π_R) and measured on Machine Ref. Plane, π_X.

γ_y= back rake: angle of inclination of the rake surface from the reference plane and measured on Machine Transverse plane, π_Y.

• Clearance angles: [Fig. 1.5]

α_x= side clearance: angle of inclination of the principal flank from the machined surface ($\overline{V_C}$) and measured on π_X plane.

α_y= back clearance: same as α_x but measured on π_Y plane.

• Cutting angles: [Fig. 1.5]

φ_s= approach angle: angle between the principal cutting edge (its projection on π_R) and π_Y and measured on π_R

φ_e= end cutting edge angle: angle between the end cutting edge (its projection on π_R) from π_X and measured on π_R

• Nose radius, r (in inch)

r = nose radius: curvature of the tool tip. It provides strengthening of the tool nose and better surface finish

• Tool Reference Systems

- **Orthogonal Rake System – ORS**

This system is also known as ISO – old.

The planes of reference and the co-ordinate axes used for expressing the tool angles in ORS are: π_R- π_C- π_O and X_o- Y_o- Z_o

Which are taken in respect of the tool configuration as indicated in Fig. 1.6

Where,

π_R = Reference plane perpendicular to the cutting velocity vector, $\overline{V_C}$

π_C = cutting plane; plane perpendicular to π_R and taken along the principal cutting edge

π_O = Orthogonal plane; plane perpendicular to both π_R and π_C and the axes;

X_o= along the line of intersection of π_R and π_O

Y_o= along the line of intersection of π_R and π_C

Z_o= along the velocity vector, i.e., normal to both X_o and Y_o axes.

The main geometrical angles used to express tool geometry in Orthogonal Rake System (ORS) and their definitions will be clear from Fig.1.7.

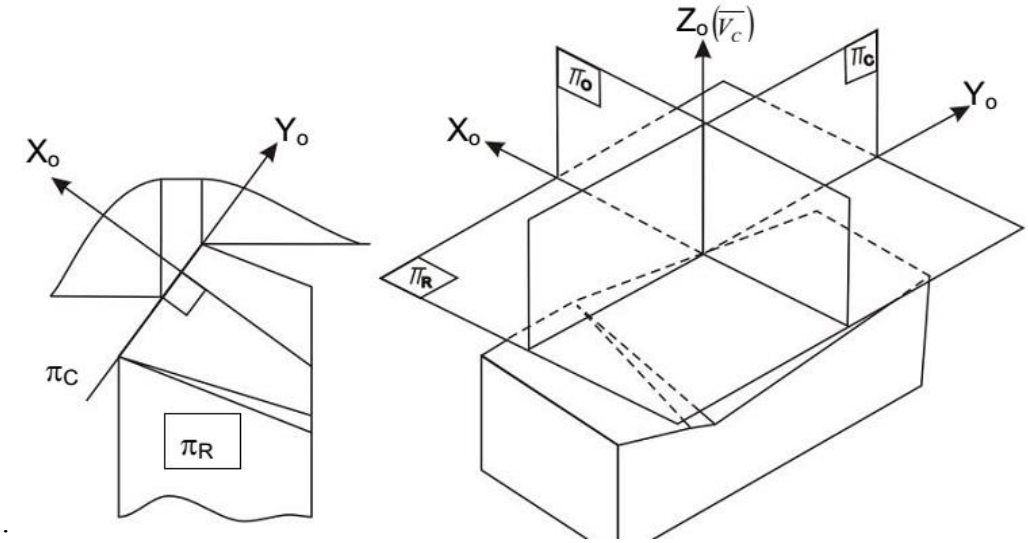

Fig. 1.6 Planes and axes of reference in ORS

Definition of –

• Rake angles [Fig. 1.7] in ORS

γ_o = orthogonal rake: angle of inclination of the rake surface from Reference plane, π_R and measured on the orthogonal plane, π_o

λ= inclination angle; angle between π_C from the direction of assumed longitudinal feed π_X and measured on π_C

• Clearance angles [Fig. 1.7]

α_o = orthogonal clearance of the principal flank: angle of inclination of the principal flank from π_C and measured on π_o

α_o'= auxiliary orthogonal clearance: angle of inclination of the auxiliary flank from auxiliary cutting plane, π_C'and measured on auxiliary orthogonal plane, π_o'as indicated in Fig.1.8.

• Cutting angles [Fig.1.7]

φ = principal cutting edge angle: angle between π_C and the direction of assumed longitudinal feed or π_X and measured on π_R

φ_1= auxiliary cutting angle: angle between π_C' and π_X and measured on π_R

• Nose radius, r (mm)

r= radius of curvature of tool tip

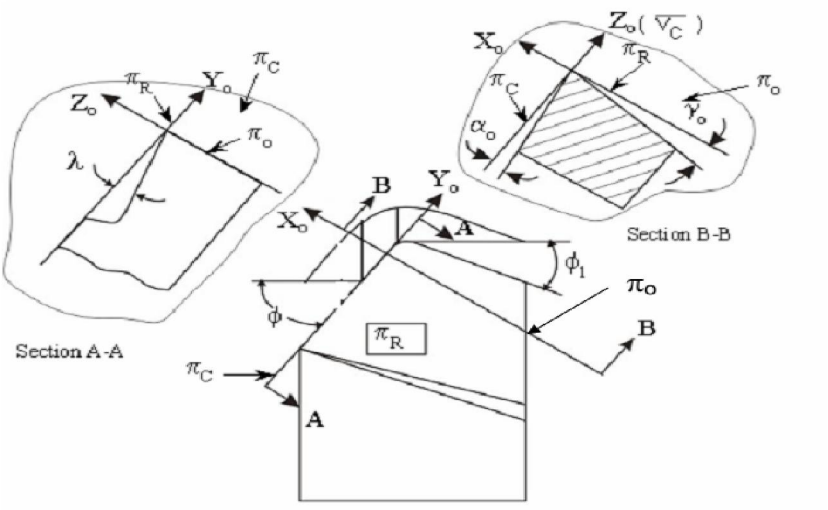

Fig. 1.7Tool angles in ORS system

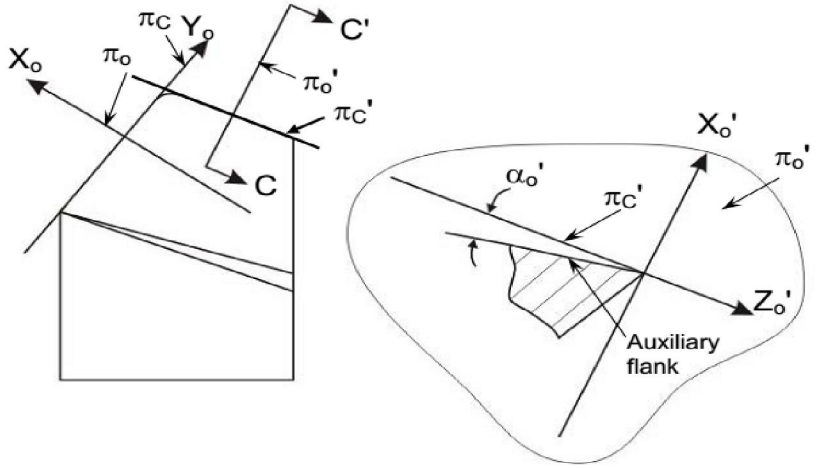

Fig. 1.8 Auxiliary orthogonal clearance angle

(b) Designation of tool geometry

The geometry of a single point tool is designated or specified by a series of values of the salient angles and nose radius arranged in a definite sequence as follows:

Designation (signature) of tool geometry in

• ASA System –

γ_y-γ_x-α_y-α_x-φ_e-φ_s-r (inch)

• ORS System –

λ-γ_o-α_o-α_o'-φ_1-φ,-r (mm)

Methods of conversion of tool angles from one system to another

- Analytical (geometrical) method: simple but tedious
- Graphical method – Master line principle: simple, quick and popular
- Transformation matrix method: suitable for complex tool geometry
- Vector method: very easy and quick but needs concept of vectors

Conversion of tool angles by Graphical method – Master Line principle.

This convenient and popular method of conversion of tool angles from ASA to ORS and vice-versa is based on use of Master Lines (ML) for the rake surface and the clearance surfaces.

• Conversion of rake angles

The concept and construction of ML for the tool rake surface is shown in Fig.1.9.

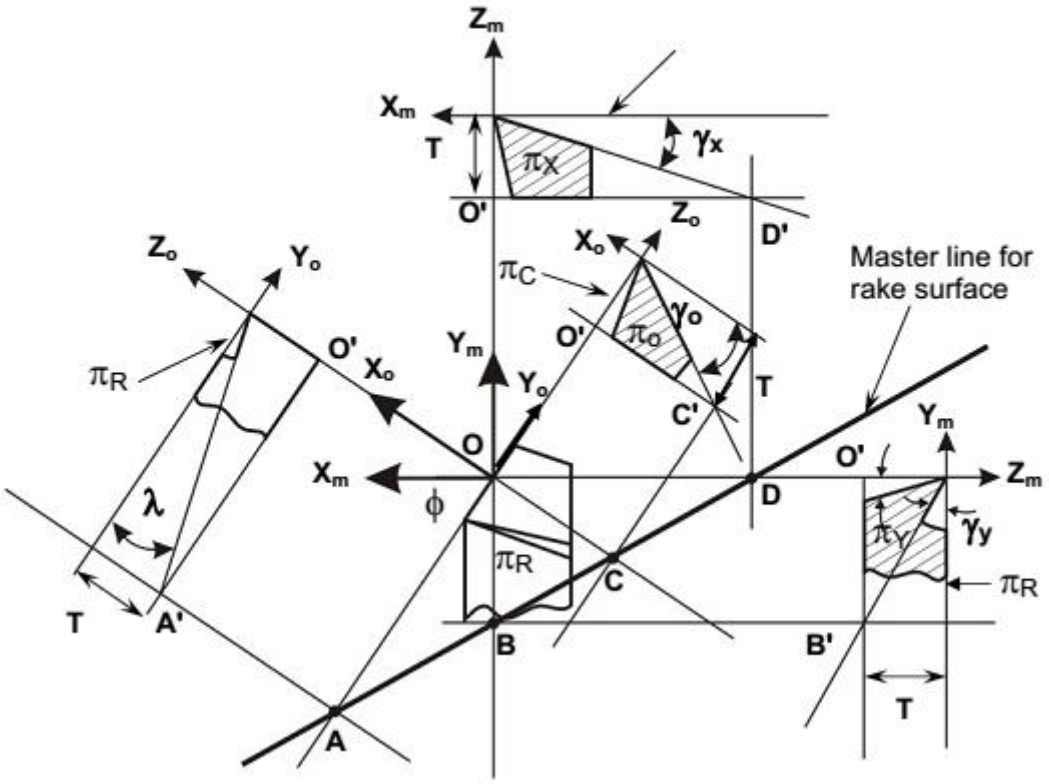

Fig. 1.9 Master line for rake surface (with all rake angles: positive)

In Fig. 1.9, the rake surface, when extended along π_X plane, meets the tool's bottom surface (which is parallel to π_R) at point D' i.e. D in the plan view. Similarly when the same tool rake surface is extended along π_Y, it meets the tool's bottom surface at point B' i.e., at B in plain view. Therefore, the straight line obtained by joining B and D is nothing but the line of intersection of the rake surface with the tool's bottom surface which is also parallel to π_R. Hence, if the rake surface is extended in any direction, its meeting point with the tool's bottom plane must be situated on the line of intersection, i.e., BD. Thus the points C and A (in Fig. 1.9) obtained by extending the rake surface along π_o and π_C respectively upto the tool's bottom surface, will be situated on that line of intersection, BD.

This line of intersection, BD between the rake surface and a plane parallel to π_R is called the "Master line of the rake surface".

From the diagram in Fig.1.9,

$OD = T\cot\gamma_X$

$OB = T\cot\gamma_Y$

$OC = T\cot\gamma_o$

$OA = T\cot\lambda$

Where, T = thickness of the tool shank.

The diagram in Fig. 1.9 is redrawn in simpler form in Fig. 1.10, for conversion of tool angles

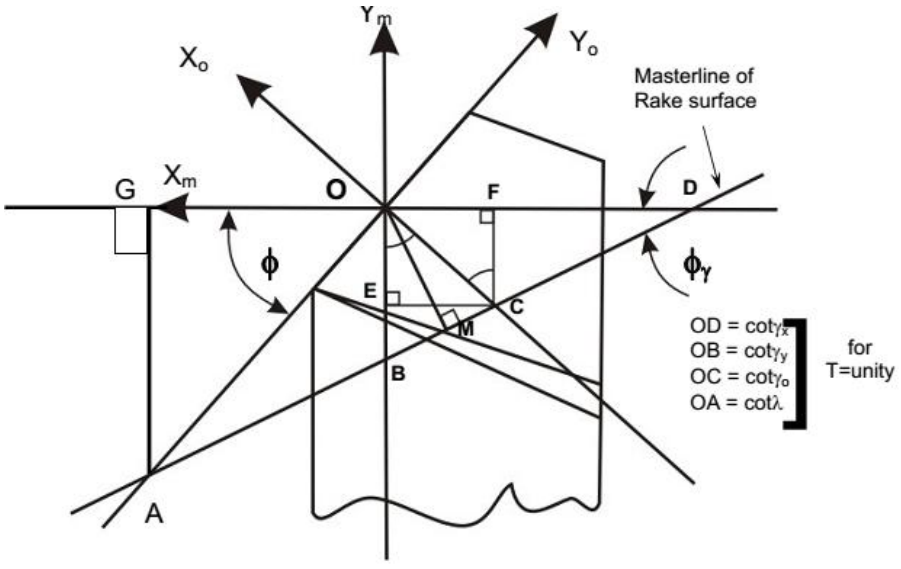

Fig. 1.10 Use of Master line for conversion of rake angles

• Conversion of tool rake angles from ASA to ORS

γ_o and λ(in ORS) = f (γ_x and γ_y of ASA system)

$$tan\gamma_0 = tan\gamma_x sin\varphi + tan\gamma_y cos\varphi \quad (1.1)$$

And $tan\lambda = -tan\gamma_x cos\varphi + tan\gamma_y sin\varphi$ (1.2)

Proof of Equation 1.1:

With respect to Fig. 1.10,

Consider, ΔOBD = ΔOBC + ΔOCD

Or, ½ OB.OD = ½ OB.CE + ½ OD.CF

Or, ½ OB.OD = ½ OB.OCsinφ+ ½ OD.OCcosφ

Dividing both sides by ½ OB.OD.OC,

$$\frac{1}{OC} = \frac{1}{OD} sin\varphi + \frac{1}{\text{OB}} \cos\varphi$$

I.e. $tan\gamma_0 = tan\gamma_x sin\varphi + tan\gamma_y cos\varphi$ ***proved***

Similarly Equation 1.2 can be proved considering;

ΔOAD = ΔOAB + ΔOBD

i.e., ½ OD.AG = ½ OB.OG + ½ OB.OD

Where, AG = OA sinφ And OG = OA cosφ

Now dividing both sides by ½ OA.OB.OD

$$\frac{1}{OB} sin\varphi = \frac{1}{OD} \cos\varphi + \frac{1}{\text{OA}}$$

i.e. $tan\lambda = -tan\gamma_x cos\varphi + tan\gamma_y sin\varphi$ ***proved***

The conversion equations 1 and 2 can be combined in a matrix form,

$$\begin{bmatrix} tan\gamma_0 \\ tan\lambda \end{bmatrix} = \begin{bmatrix} sin\varphi & \cos\varphi \\ -\cos\varphi & sin\varphi \end{bmatrix} \begin{bmatrix} tan\gamma_x \\ tan\gamma_y \end{bmatrix} \quad (1.3)$$

(ORS) (ASA)

Where, $\begin{bmatrix} sin\varphi & \cos\varphi \\ -\cos\varphi & sin\varphi \end{bmatrix}$ is the transformation matrix.

• Conversion of rake angles from ORS to ASA system

γ_x and γ_y (in ASA) = f(γ_o and λ of ORS)

$$tan\gamma_x = \tan\gamma_0 sin\varphi - \tan\lambda\cos\varphi \quad (1.4)$$

$$tan\gamma_y = \tan\gamma_0 cos\varphi + \tan\lambda\cos\varphi \quad (1.5)$$

The relations (1.4) and (1.5) can be arrived at indirectly using Equation 3.

By inversion, Equation 3 becomes, (1.6)

$$\begin{bmatrix} tan\gamma_x \\ tan\gamma_y \end{bmatrix} = \begin{bmatrix} sin\varphi & -\cos\varphi \\ \cos\varphi & sin\varphi \end{bmatrix} \begin{bmatrix} tan\gamma_0 \\ tan\lambda \end{bmatrix} \quad (1.6)$$

(ASA) (ORS)

Conversion of clearance angles from ASA system to ORS and vice versa by Graphical method.

Like rake angles, the conversion of clearance angles also make use of corresponding Master lines. The Master lines of the two flank surfaces are nothing but the dotted lines that appear in the plan view of the tool (Fig. 1.11). The dotted line are the lines of intersection of the flank surfaces concerned with the tool's bottom surface which is parallel to the Reference plane π_R.

Thus according to the definition those two lines represent the Master lines of the flank surfaces.

Fig. 1.12 shows the geometrical features of the Master line of the principal flank of a single point cutting tool.

From Fig. 1.12,

OD = T$\tan\alpha_x$

OB = T$\tan\alpha_y$

OC = T$\tan\alpha_o$

OA = T$\cot\lambda$ where, T = thickness of the tool shank.

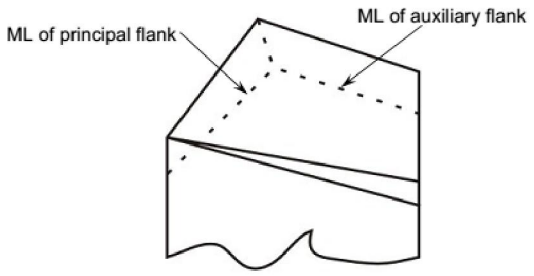

Fig. 1.11 Master lines (ML) of flank surfaces

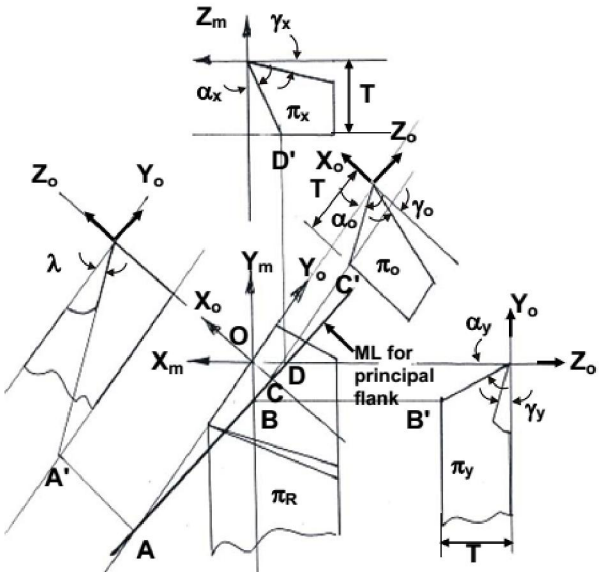

Fig. 1.12 Master line of principal flank.

The diagram in Fig. 1.12 is redrawn in simpler form in Fig. 1.13 for conversion of clearance angles. The inclination angle, λ basically represents slope of the rake surface along the principal cutting edge and hence is considered as a rake angle. But λ appears in the analysis of clearance angles also because the principal cutting edge belongs to both the rake surface and the principal flank.

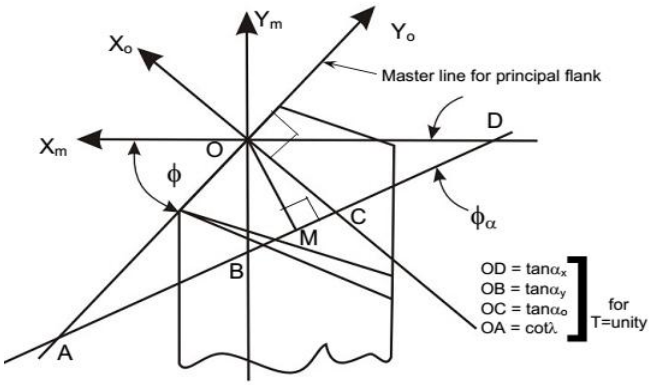

Fig. 1.13 Use of Master line for conversion of clearance angles

• Conversion of clearance angles from ASA to ORS

Angles, α_o and λ in ORS = f(α_x and α_y in ASA system)

Following the same way used for converting the rake angles taking suitable triangles, the following expressions can be arrived at using Fig. 1.13:

$$cot\alpha_0 = cot\alpha_x sin\varphi + \cot\alpha_y \cos\varphi$$

$$tan\lambda = -cot\alpha_x \cos\varphi + \cot\alpha_y sin\varphi$$

• Conversion of clearance angles from ORS to ASA system

α_x and α_y (in ASA) = f(α_o and λ in ORS)

Proceeding in the same way using Fig.13, the following expressions are derived

$$cot\alpha_x = cot\alpha_0 sin\varphi - tan\lambda \cos\varphi$$

$$tan\alpha_y = cot\alpha_0 \cos\varphi + tan\lambda sin\varphi$$

Mechanism of chip formation in machining

Machining is a semi-finishing or finishing process essentially done to impart required or stipulated dimensional and form accuracy and surface finish to enable the product to

• fulfill its basic functional requirements

• provide better or improved performance

• render long service life.

Machining is a process of gradual removal of excess material from the preformed blanks in the form of chips. The form of the chips is an important index of machining because it directly or indirectly indicates:

• Nature and behavior of the work material under machining condition

• Specific energy requirement (amount of energy required to remove unit volume of work material) in machining work

• Nature and degree of interaction at the chip-tool interfaces.

The form of machined chips depends mainly upon:

•Work material

• Material and geometry of the cutting tool

• Levels of cutting velocity and feed and also to some extent on depth of cut

• Machining environment or cutting fluid that affects temperature and friction at the chip-tool and work-tool interfaces

Knowledge of basic mechanism(s) of chip formation helps to understand the characteristics of chips and to attain favorable chip forms.

• **Mechanism of chip formation in machining ductile materials**

During continuous machining the uncut layer of the work material just ahead of the cutting tool (edge) is subjected to almost all sided compression as indicated in Fig. 1.14.

The force exerted by the tool on the chip arises out of the normal force, N and frictional force, F as indicated in Fig. 1.14. Due to such compression, shear stress develops, within that compressed region, in different magnitude, in different directions and rapidly increases in magnitude. Whenever and wherever the value of the shear stress reaches or exceeds the shear strength of that work material in the deformation region, yielding or slip takes place resulting shear deformation in that region and the plane of maximum shear stress. But the forces causing the shear stresses in the region of the chip quickly diminishes and finally disappears while that region moves along the tool rake surface towards and then goes beyond the point of chip-tool engagement. As a result the slip or shear stops propagating long before total separation takes place.

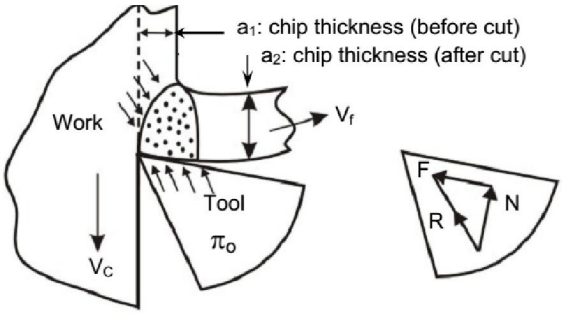

Fig. 1.14 Compression of work material (layer) ahead of the tool tip

In the mean time the succeeding portion of the chip starts undergoing compression followed by yielding and shear. This phenomenon repeats rapidly resulting in formation and removal of chips in thin layer by layer. This phenomenon has been explained in a simple way by using a card analogy as shown in Fig. 1.15.

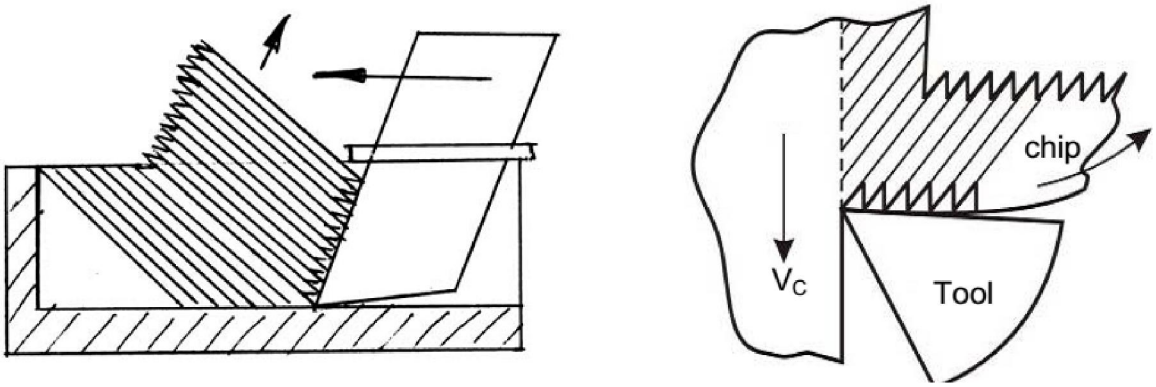

(a) Shifting of the postcards by partial sliding against each other (b) Chip formation by shear in lamella

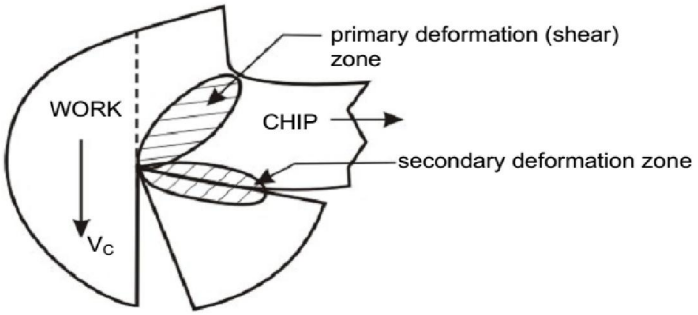

Fig.1. 15 Primary and secondary deformation zones in the chip.

In actual machining chips also, such serrations are visible at their upper surface as indicated in Fig. 1.15. The lower surface becomes smooth due to further plastic deformation due to intensive rubbing with the tool at high pressure and temperature. The pattern of shear deformation by lamellar sliding, indicated in the model, can also be seen in actual chips by proper mounting, etching and polishing the side surface of the machining chip and observing under microscope.

The pattern and extent of total deformation of the chips due to the primary and the secondary shear deformations of the chips ahead and along the tool face, as indicated in Fig. 15, depend upon

•work material

• Tool material and geometry

• The machining speed (V_C) and feed (s_o)

• cutting fluid application

The overall deformation process causing chip formation is quite complex and hence needs thorough experimental studies for clear understanding the phenomena and its dependence on the affecting parameters. The feasible and popular experimental methods for this purpose are:

• Study of deformation of rectangular or circular grids marked on the side surface as shown in Fig. 16

• Microscopic study of chips frozen by drop tool or quick stop apparatus

• Study of running chips by high speed camera fitted with low magnification microscope.

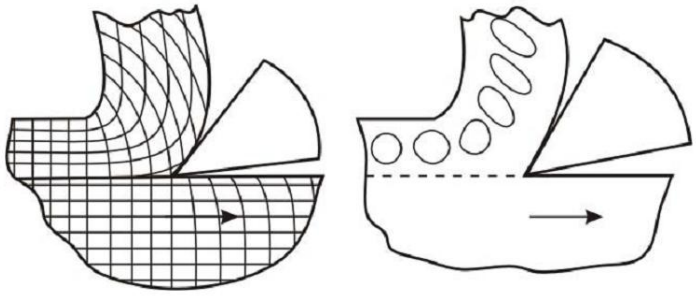

(a) Rectangular grids (b) circular grids

Fig. 1.16 Pattern of grid deformation during chip formation.

It has been established by several analytical and experimental methods including circular grid deformation that though the chips are initially compressed ahead of the tool tip, the final

deformation is accomplished mostly by shear in machining ductile materials. However, machining of ductile materials generally produces flat, curved or coiled continuous chips.

• Mechanism of chip formation in machining brittle materials

The basic two mechanisms involved in chip formation are

• Yielding – generally for ductile materials

• Brittle fracture – generally for brittle materials

During machining, first a small crack develops at the tool tip as shown in Fig.1.17 due to wedging action of the cutting edge. At the sharp crack-tip stress concentration takes place. In case of ductile materials immediately yielding takes place at the crack-tip and reduces the effect of stress concentration and prevents its propagation as crack. But in case of brittle materials the initiated crack quickly propagates, under stressing action, and total separation takes place from the parent work piece through the minimum resistance path as indicated in Fig. 1.17.

Machining of brittle material produces discontinuous chips and mostly of irregular size and shape. The process of forming such chips is schematically shown in Fig. 1.18.

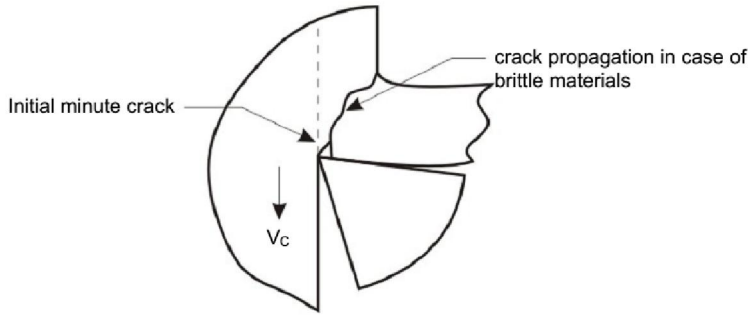

Fig. 1.17 Development and propagation of crack causing chip separation.

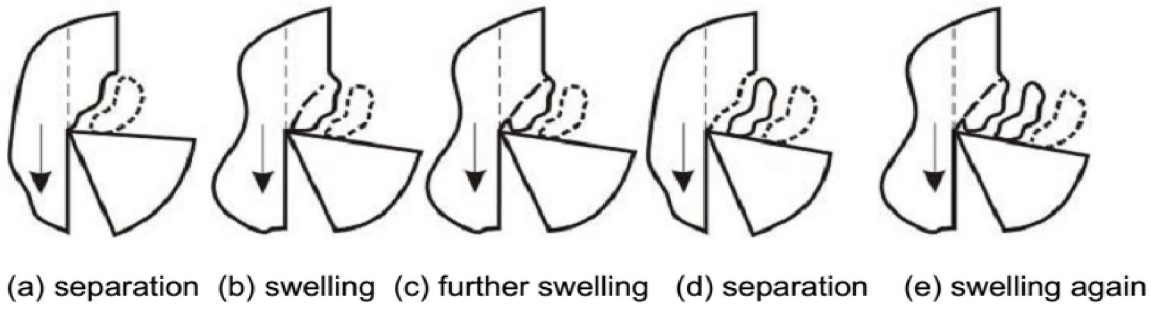

Fig. 1.18 Schematic view of chip formation in machining brittle materials.

Geometry and characteristics of chip forms

The geometry of the chips being formed at the cutting zone follow a particular pattern especially in machining ductile materials. The major sections of the engineering materials being machined are ductile in nature, even some semi ductile or semi-brittle materials behave ductile under the compressive forces at the cutting zone during machining. The pattern and degree of deformation during chip formation are quantitatively assessed and expressed by some factors, the values of which indicate about the forces and energy required for a particular machining work.

• Chip reduction coefficient or cutting ratio

The usual geometrical features of formation of continuous chips are schematically shown in Fig. 1.19.

The chip thickness (a_2) usually becomes larger than the uncut chip thickness (a_1). The reason can be attributed to

• Compression of the chip ahead of the tool

• Frictional resistance to chip flow

• Lamellar sliding

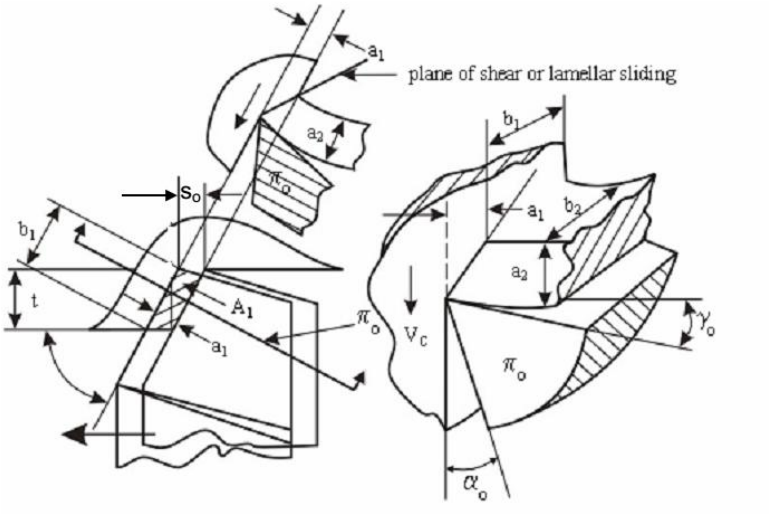

Fig. 1.19 Geometrical features of continuous chips' formation.

The significant geometrical parameters involved in chip formation are shown in Fig. 1.19 and those parameters are defined (in respect of straight turning) as:

t = depth of cut (mm) – perpendicular penetration of the cutting tool tip in work surface

s_o= feed (mm/rev) – axial travel of the tool per revolution of the job

b_1= width (mm) of chip before cut

b_2= width (mm) of chip after cut

a_1= thickness (mm) of uncut layer (or chip before cut)

a_2= chip thickness (mm) – thickness of chip after cut

A1= cross section (area, mm^2) of chip before cut

The degree of thickening of the chip is expressed by

$\frac{a_2}{a_1} = \zeta > 1.00$ (since $a_2 > a_1$) (1.7)

Where, ζ= chip reduction coefficient

$a_1 = s_o \sin\varphi$ (1.8)

Where φ= principal cutting edge angle

Larger value of ζ means more thickening i.e., more effort in terms of forces or energy required to accomplish the machining work. Therefore it is always desirable to reduce a_2 or ζ without sacrificing productivity, i.e. metal removal rate (MRR).

Chip thickening is also often expressed by the reciprocal of ζ as,

$$\frac{1}{\zeta} = r = \frac{a_1}{a_2} \quad (1.9)$$

Where, r = cutting ratio

The value of chip reduction coefficient, ζ (and hence cutting ratio) depends mainly upon

• Tool rake angle, γ

• Chip-tool interaction, mainly friction, μ

Roughly in the following way

$\zeta = \mu^{(\frac{\pi}{2} - \gamma o)}$ [for orthogonal cutting] (1.10)

Π/2 and γ_o are in radians

The simple but very significant expression (1.10) clearly depicts that the value of ζ can be desirably reduced by

• Using tool having larger positive rake

• Reducing friction by using lubricant

The role of rake angle and friction at the chip-tool interface on chip reduction coefficient are also schematically shown in Fig. 1.20.

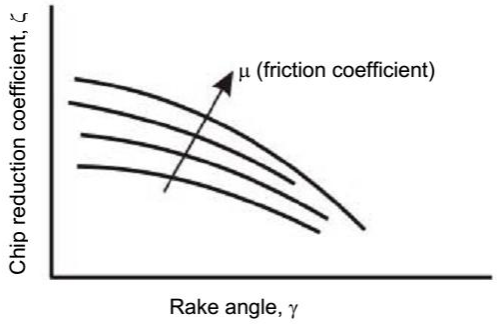

Fig. 1.20 Role of rake angle and friction on chip reduction coefficient

Chip reduction coefficient, ζ is generally assessed and expressed by the ratio of the chip thickness, after (a_2) and before cut (a_1) as in equation 1.7. But ζ can also be expressed or assessed by the ratio of Considering total volume of chip produced in a given time,

$$a_1 b_1 L_1 = a_2 b_2 L_2 \quad (1.11)$$

The width of chip, b generally does not change significantly during machining unless there is side flow for some adverse situation. Therefore assuming, $b_1=b_2$ in equation (1.11), ζ comes up to be,

$$\frac{a_2}{a_1} = \zeta = \frac{L_1}{L_2} \quad (1.12)$$

Again considering unchanged material flow (volume) ratio, Q

$$Q = (a_1 b_1)V_C = (a_2 b_2)V_f \quad (1.13)$$

Taking $b_1=b_2$,

$$\frac{a_2}{a_1} = \zeta = \frac{V_C}{V_f} \quad (1.14)$$

Equation (1.14) reveals that the chip velocity, V_f will be lesser than the cutting velocity, V_C and the ratio is equal to the cutting ratio, $r = \frac{1}{\zeta}$

• Shear angle

It has been observed that during machining, particularly ductile materials, the chip sharply changes its direction of flow (relative to the tool) from the direction of the cutting velocity, V_C to that along the tool rake surface after thickening by shear deformation or slip or lamellar sliding along a plane. This plane is called shear plane

Shear plane: Shear plane is the plane of separation of work material layer in the form of chip from the parent body due to shear along that plane.

Shear angle: Angle of inclination of the shear plane from the direction of cutting velocity.

The value of shear angle, denoted by β_o(taken in orthogonal plane) depends upon

• Chip thickness before and after cut i.e. ζ

•Rake angle, γ_o(in orthogonal plane)

From Fig. 1.21,

$AC = a_2 = OA\cos(\beta_o - \gamma_o)$

And $AB = a_1 = OA\sin\beta_o$

Dividing a_2 by a_1

$$\frac{a_2}{a_1} = \zeta = \frac{\cos(\beta_0 - \gamma_0)}{\sin\beta_0} \quad (1.15)$$

$$\text{Or } tan\beta_0 = \frac{\cos\gamma_0}{\zeta - \sin\gamma_0} \quad (1.16)$$

Replacing chip reduction coefficient, ζ by cutting ratio, r, the equation (1.16) changes to

$$tan\beta_0 = \frac{r\cos\gamma_0}{1 - r\sin\gamma_0} \quad (1.17)$$

Equation 1.16 depicts that with the increase in ζ, shear angle decreases and vice-versa. It is also evident from equation (1.16) that shear angle increases both directly and indirectly with the increase in tool rake angle. Increase in shear angle means more favourable machining condition requiring lesser specific energy.

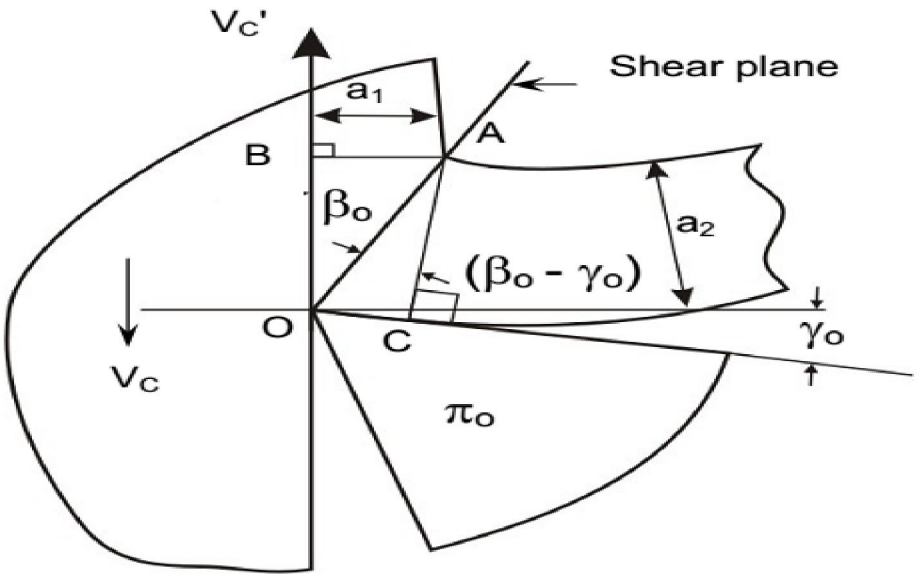

Fig. 1.21 Shear plane and shear angle in chip formation

• Cutting strain

The magnitude of strain, that develops along the shear plane due to machining action, is called cutting strain (shear). The relationship of this cutting strain, ε with the governing parameters can be derived from Fig. 1.22. Due to presence of the tool as an obstruction the layer 1 has been shifted to position 2 by sliding along the shear plane.

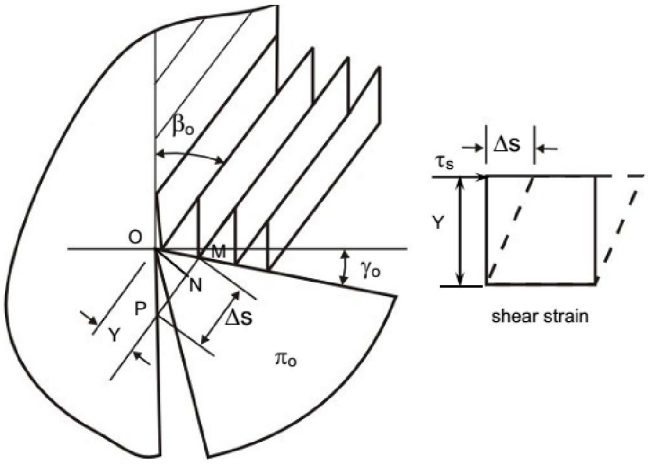

Fig.1.22 Cutting strain in machining

From Fig. 1.22,

Cutting strain (average),

$\varepsilon = \frac{\Delta s}{y} = \frac{PM}{ON}$

Or, $\varepsilon = \frac{PN}{ON} + \frac{NM}{ON}$

$$\varepsilon = \cot\beta_0 + \tan(\beta_0 - \gamma_0) \quad (1.18)$$

(Iii) built-up-Edge (BUE) formation

• Causes of formation

In machining ductile metals like steels with long chip-tool contact length, lot of stress and temperature develops in the secondary deformation zone at the chip-tool interface. Under such high stress and temperature in between two clean surfaces of metals, strong bonding may locally take place due to adhesion similar to welding. Such bonding will be encouraged and accelerated if the chip tool materials have mutual affinity or solubility. The weldment starts forming as an embryo at the most favourable location and thus gradually grows as schematically shown in Fig. 1.23.

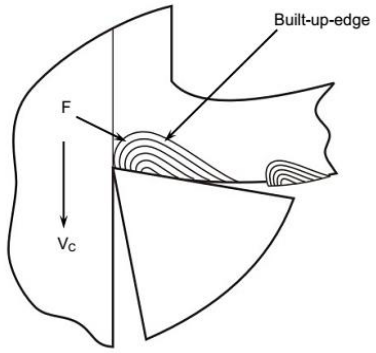

Fig. 1.23 Scheme of built-up-edge formation

With the growth of the BUE, the force,F (shown in Fig. 1.23) also gradually increases due to wedging action of the tool tip along with the BUE formed on it. Whenever the force, F exceeds the bonding force of the BUE, the BUE is broken or sheared off and taken away by the flowing chip. Then again BUE starts forming and growing. This goes on repeatedly.

• Characteristics of BUE

Built-up-edges are characterized by its shape, size and bond strength, which depend upon:

• work tool materials

• Stress and temperature, i.e., cutting velocity and feed

• cutting fluid application governing cooling and lubrication.

BUE may develop basically in three different shapes as schematically shown in Fig. 1.24.

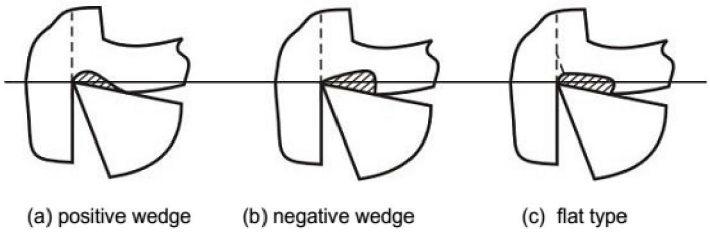

Fig. 1.24 Different forms of built-up-edge.

In machining too soft and ductile metals by tools like high speed steel or uncoated carbide the BUE may grow larger and overflow towards the finished surface through the flank as shown in Fig. 1.24

While the major part of the detached BUE goes away along the flowing chip, a small part of the BUE may remain stuck on the machined surface and spoils the surface finish. BUE formation needs certain level of temperature at the interface depending upon the mutual affinity of the work-tool materials. With the increase in V_C and so the cutting temperature rises and favours BUE formation. But if V_C is raised too high beyond certain limit, BUE will be squashed out by the flowing chip before the BUE grows. Fig. 1.25 shows schematically the role of increasing V_C and soon BUE formation (size). But sometime the BUE may adhere so strongly that it remains strongly bonded at the tool tip and does not break or shear off even after reasonably long time of machining. Such detrimental situation occurs in case of certain tool-work materials and at speed-feed conditions which strongly favour adhesion and welding.

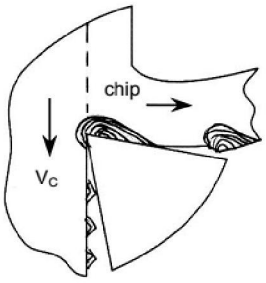

Fig. 1.24Overgrowing and overflowing of BUE causing surface roughness

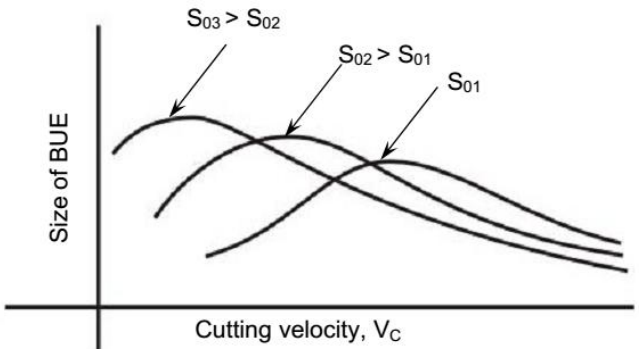

Fig. 1.25 Role of cutting velocity and feed on BUE formation.

• **Effects of BUE formation**

Formation of BUE causes several harmful effects, such as:

• It unfavorably changes the rake angle at the tool tip causing increase in cutting forces and power consumption

• Repeated formation and dislodgement of the BUE causes fluctuation in cutting forces and thus induces vibration which is harmful for the tool, job and the machine tool.

• Surface finish gets deteriorated

• May reduce tool life by accelerating tool-wear at its rake surface by adhesion and flaking

Occasionally, formation of thin flat type stable BUE may reduce tool wear at the rake face.

Types of chips and conditions for formation of those chips

Different types of chips of various shape, size, colour etc. are produced by machining depending upon

• Type of cut, i.e., continuous (turning, boring etc.) or intermittent cut (milling)

• Work material (brittle or ductile etc.)

• Cutting tool geometry (rake, cutting angles etc.)

• Levels of the cutting velocity and feed (low, medium or high)

• cutting fluid (type of fluid and method of application)

The basic major types of chips and the conditions generally under which such types of chips form are given below:

Discontinuous type

• Of irregular size and shape: - work material – brittle like grey cast iron

• Of regular size and shape: - work material ductile but hard and work hardenable

- Feed – large

- Tool rake – negative

- Cutting fluid – absent or inadequate

Continuous type

• Without BUE:

Work material – ductile

Cutting velocity – high

Feed – low

Rake angle – positive and large

Cutting fluid – both cooling and lubricating

• With BUE:

- Work material – ductile

- Cutting velocity – medium

- Feed – medium or large

- cutting fluid – inadequate or absent.

Often in machining ductile metals at high speed, the chips are deliberately broken into small segments of regular size and shape by using chip breakers mainly for convenience and reduction of chip-tool contact length.

Tool materials.

The capability and overall performance of the cutting tools depend upon,

• The cutting tool materials

• The cutting tool geometry

• Proper selection and use of those tools

• The machining conditions and the environments

Out of which the tool material plays the most vital role.

Characteristics and Applications of the Primary Cutting Tool Materials

(a) High Speed Steel (HSS)

Advent of HSS in around 1905 made a break through at that time in the history of cutting tool materials though got later superseded by many other novel tool materials like cemented carbides and ceramics which could machine much faster than the HSS tools.

The basic composition of HSS is 18% W, 4% Cr, 1%V, 0.7% C and rest Fe.

Such HSS tool could machine (turn) mild steel jobs at speed only up to 20 ~ 30 m/min (which was quite substantial those days) However, HSS is still used as cutting tool material where;

• the tool geometry and mechanics of chip formation are complex, such as helical twist drills, reamers, gear shaping cutters, hobs, form tools, broaches etc.

• Brittle tools like carbides, ceramics etc. are not suitable under shock loading

• The small scale industries cannot afford costlier tools

• The old or low powered small machine tools cannot accept high speed and feed.

• The tool is to be used number of times by resharpening.

With time the effectiveness and efficiency of HSS (tools) and their application range were gradually enhanced by improving its properties and surface condition through -

• Refinement of microstructure

• Addition of large amount of cobalt and Vanadium to increase hot hardness and wear resistance respectively

• Manufacture by powder metallurgical process

• Surface coating with heat and wear resistive materials like TiC, TiN, etc by Chemical Vapour Deposition (CVD) or Physical Vapor Deposition (PVD)

Addition of large amount of Co and V, refinement of microstructure and coating increased strength and wear resistance and thus enhanced productivity and life of the HSS tools remarkably.

(b) Stellite

This is a cast alloy of Co (40 to 50%), Cr (27 to 32%), W (14 to 19%) and C (2%). Stellite is quite tough and more heat and wear resistive than the basic HSS (18 – 4 – 1) But such stellite as cutting tool material became obsolete for its poor grind ability and especially after the arrival of cemented carbides.

(c) Sintered Tungsten carbides

The advent of sintered carbides made another breakthrough in the history of cutting tool materials.

• Straight or single carbide

First the straight or single carbide tools or inserts were powder metallurgically produced by mixing, compacting and sintering 90 to 95% WC powder with cobalt. The hot, hard and wear resistant WC grains are held by the binder Co which provides the necessary strength and toughness. Such tools are suitable for machining grey cast iron, brass, bronze etc. which produce short discontinuous chips and at cutting velocities two to three times of that possible for HSS tools.

• Composite carbides

The single carbide is not suitable for machining steels because of rapid growth of wear, particularly crater wear, by diffusion of Co and carbon from the tool to the chip under the high stress and temperature bulk (plastic) contact between the continuous chip and the tool surfaces. For machining steels successfully, another type called composite carbide have been developed by adding (8 to 20%) a gamma phase to WC and Co mix. The gamma phase is a mix of TiC, TiN, TaC, NiC etc. which are more diffusion resistant than WC due to their more stability and less wettability by steel.

• Mixed carbides

Titanium carbide (TiC) is not only more stable but also much harder than WC. So for machining ferritic steels causing intensive diffusion and adhesion wear a large quantity (5 to 25%) of TiC is added with WC and Co to produce another grade called mixed carbide. But increase in TiC content reduces the toughness of the tools. Therefore, for finishing with light cut but high speed, the harder grades containing upto 25% TiC are used and for heavy roughing work at lower speeds lesser amount (5 to 10%) of TiC is suitable.

(d) Plain ceramics

Inherently high compressive strength, chemical stability and hot hardness of the ceramics led to powder metallurgical production of index able ceramic tool inserts since 1950. Alumina (Al_2O_3) is preferred to silicon nitride (Si3N4) for higher hardness and chemical stability. $Si_3N_4$is tougher but again more difficult to process. The plain ceramic tools are brittle in nature and hence had limited applications.

Basically three types of ceramic tool bits are available in the market;

• Plain alumina with traces of additives – these white or pink sintered inserts are cold pressed and are used mainly for machining cast iron and similar materials at speeds 200 to 250 m/min

• Alumina; with or without additives – hot pressed, black colour, hard and strong – used for machining steels and cast iron at VC= 150 to 250 m/min

• Carbide ceramic (Al2O3+ 30% TiC) cold or hot pressed, black colour, quite strong and enough tough – used for machining hard cast irons and plain and alloy steels at 150 to 200 m/min.

However, the use of those brittle plain ceramic tools, until their strength and toughness could be substantially improved since 1970, gradually decreased for being restricted to

• Uninterrupted machining of soft cast irons and steels only

• Relatively high cutting velocity but only in a narrow range (200 ~ 300 m/min)

• requiring very rigid machine tools

Advent of coated carbide capable of machining cast iron and steels at high velocity made the then ceramics almost obsolete.

(e)Cermets

These sintered hard inserts are made by combining ‘cer’ from ceramics like TiC, TiN orn(or)TiCN and ‘met’ from metal (binder) like Ni, Ni-Co, Fe etc. Since around 1980, the modern cermets providing much better performance are being made by TiCN which is consistently more wear resistant, less porous and easier to make. The characteristic features of such cermets, in contrast to sintered tungsten carbides, are:

• The grains are made of TiCN (in place of WC) and Ni or Ni-Co and Fe as binder (in place of Co)

• Harder, more chemically stable and hence more wear resistant

• More brittle and less thermal shock resistant

• Wt% of binder metal varies from 10 to 20%

• Cutting edge sharpness is retained unlike in coated carbide inserts

• Can machine steels at higher cutting velocity than that used for tungsten carbide, even coated carbides in case of light cuts.

Application wise, the modern TiCN based cermets with bevelled or slightly rounded cutting edges are suitable for finishing and semi-finishing of steels at higher speeds, stainless steels but are not suitable for jerky interrupted machining and machining of aluminum and similar materials. Research and development are still going on for further improvement in the properties and performance of cermets.

(f)Coronite

It is already mentioned earlier that the properties and performance of HSS tools could have been sizeably improved by refinement of microstructure, powder metallurgical process of making and surface coating. Recently a unique tool material, namely Coronite has been developed for making the tools like small and mediumsize drills and milling cutters etc. which were earlier essentially made of HSS. Coronite is made basically by combining HSS for strength and toughness and tungsten carbides for heat and wear resistance. Micro fine TiCN particles are uniformly dispersed into the matrix.

Unlike solid carbide, the coronate based tool is made of three layers;

• The central HSS or spring steel core

• A layer of coronite of thickness around 15% of the tool diameter

• A thin (2 to 5 μm) PVD coating of TiCN.

Such tools are not only more productive but also provide better product quality. The coronite tools made by hot extrusion followed by PVD-coatring of TiN or TiCN outperformed HSS tools in respect of cutting forces, tool life and surface finish.

(g) High Performance ceramics (HPC)

Ceramic tools as such are much superior to sintered carbides in respect of hot hardness, chemical stability and resistance to heat and wear but lack in fracture toughness and strength. Through last fewyears remarkable improvements in strength and toughness and hence overall performance of ceramic tools could have been possible by several means which include;

•Sinterability, microstructure, strength and toughness of Al2O3ceramics were improved to some extent by adding TiO2and MgO

• Transformation toughening by adding appropriate amount of partially or fully stabilised zirconia in Al2O3powder

• Isostatic and hot isostatic pressing (HIP) – these are very effective but expensive route.

• Introducing nitride ceramic (Si3N4) with proper sintering technique – this material is very tough but prone to built-up-edge formation in machining steels

• Developing SIALON – deriving beneficial effects of Al2O3and Si3N4

• Adding carbide like TiC (5 ~ 15%) in Al2O3powder – to impart toughness and thermal conductivity

• Reinforcing oxide or nitride ceramics by SiC whiskers, which enhanced strength, toughness and life of the tool and thus productivity spectacularly. But manufacture and use of this unique tool need specially careful handling

•Toughening Al2O3ceramic by adding suitable metal like silver which also impart thermal conductivity and self lubricating property; this novel and inexpensive tool is still in experimental stage.

The enhanced qualities of the unique high performance ceramic tools, specially the whisker and zirconia based types enabled them machine structural steels at speed even beyond 500 m/min and also intermittent cutting at reasonably high speeds, feeds and depth of cut. Such tools are also found to machine relatively harder and stronger steels quite effectively and economically.

Nitride based ceramic tools

Plain nitride ceramics tools

Compared to plain alumina ceramics, Nitride (Si3N4) ceramic tools exhibit more resistance to fracturing by mechanical and thermal shocks due to higher bending strength, toughness and higher conductivity. Hence such tool seems to be more suitable for rough and interrupted cutting of various material excepting steels, which cause rapid diffusional wear and BUE formation. The fracture toughness and wear resistance of nitride ceramic tools could be further increased by adding zirconia and coating the finished tools with high hardness alumina and titanium compound. Nitride ceramics cannot be easily compacted and sintered to high density. Sintering with the aid of ‘reaction bonding’ and ‘hot pressing’ may reduce this problem to some extent.

SIALON tools

Hot pressing and sintering of an appropriate mix of Al_2O_3 and Si_3N_4 powders yielded an excellent composite ceramic tool called SIALON which are very hot hard, quite tough and wear resistant. These tools can machine steel and cast irons at high speeds (250 – 300 m/min). But machining of steels by such tools at too high speeds reduces the tool life by rapid diffusion.

SiC reinforced Nitride tools

The toughness, strength and thermal conductivity and hence the overall performance of nitride ceramics could be increased remarkably by adding SiC whiskers or fibers in 5 – 25 volume%. The SiC whsikers add fracture toughness mainly through crack bridging, crack deflection and fiber pull-out Such tools are very expensive but extremely suitable for high production machining of various soft and hard materials even under interrupted cutting.

Zirconia (or partially stabilized Zirconia) toughened alumina (ZTA) ceramic

The enhanced strength, TRS and toughness have made these ZTAs more widely applicable and more productive than plain ceramics and cermets in machining steels and cast irons. Fine powder of partially stabilised zirconia (PSZ) is mixed in proportion of ten to twenty volume percentage with pure alumina, then either cold pressed and sintered at 1600 – 1700^oC or hot isostatically pressed (HIP) under suitable temperature and pressure. The phase transformation of metastable tetragonal zirconia (t-Z) to monoclinic zirconia (m-Z) during cooling of the composite (Al2O3+ ZrO2) inserts after sintering or HIP and during polishing and machining imparts the desired strength and fracture toughness through volume expansion (3 – 5%) and induced shear strain (7%). Their hardness have been raised further by proper control of particle size and sintering process. Hot pressing and HIP raise the density, strength and hot hardness of ZTA tools but the process becomes expensive and the tool performance degrades at lower cutting speeds. However such ceramic tools can machine steel and cast iron at speed range of 150 – 500 m/min. Alumina ceramic reinforced by SiC whiskers .The properties, performances and application range of alumina based ceramic tools have been improved spectacularly through drastic increase in fracture toughness (2.5 times), TRS and bulk thermal conductivity, without sacrificing hardness and wear resistance by mechanically reinforcing the brittle alumina matrix with extremely strong and stiff silicon carbide whiskers. The randomly oriented, strong and thermally conductive whsikers enhance the strength and toughness mainly by crack deflection and crack-bridging and also by reducing the temperature gradient within the tool. After optimization of the composition, processing and the tool geometry, such tools have been found to effectively and efficiently machine wide range of materials, over wide speed range (250 – 600 m/min) even under large chip loads. But manufacturing of whiskers need very careful handling and precise control and these tools are costlier than zirconia toughened ceramic tools.

Silver toughened alumina ceramic

Toughening of alumina with metal particle became an important topic since 1990 though its possibility was reported in 1950s. Alumina-metal composites have been studied primarily using addition of metals like aluminum, nickel, chromium, molybdenum, iron and silver. Compared to zirconia and carbides, metals were found to provide more toughness in alumina ceramics. Again compared to other metal toughened ceramics, the silver-toughened ceramics can be manufactured by simpler and more economical process routes like pressure less sintering and without atmosphere control. All such potential characteristics of silver-toughened alumina ceramic have already been exploited in making some salient parts of automobiles and similar items. Research is going on to develop and use silver-toughened alumina for making cutting tools like turning inserts.. The toughening of the alumina matrix by the addition of metal occurs mainly by crack deflection and crack bridging by the metal grains as. Addition of silver further helps by increasing thermal conductivity of the tool and self lubrication by the traces of the silver that oozes out through the pores and reaches at the chip tool interface. Such HPC tools can suitably machine with large MRR and VC (250 – 400 m/min) and long tool life even under light interrupted cutting like milling. Such tools also can machine steels at speed from quite low to very high cutting velocities (200 to 500 m/min).

(h) Cubic Boron Nitride

Next to diamond, cubic boron nitride is the hardest material presently available. Only in 1970 and onward CBN in the form of compacts has been introduced as cutting tools. It is made by bonding a 0.5 – 1 mm layer of polycrystalline cubic boron nitride to cobalt based carbide substrate at very high temperature and pressure. It remains inert and retains high hardness and fracture toughness at elevated machining speeds. It shows excellent performance in grinding any material of high hardness and strength. The extreme hardness, toughness, chemical and thermal stability and wear resistance led to the development of CBN cutting tool inserts for high material removal rate (MRR) as well as precision machining imparting excellent surface integrity of the products. Such unique tools effectively and beneficially used in machining wide range of work materials covering high carbon and alloy steels, non-ferrous metals and alloys, exotic metals like Ni-hard, Inconel, Nimonic etc and many non-metallic materials which are as such difficult to machine by conventional tools. It is firmly stable at temperatures up to 1400oC. The operative speed range for CBN when machining grey cast iron is 300 ~ 400 m/min. Speed ranges for other materials are as follows:

• Hard cast iron (> 400 BHN): 80 – 300 m/min

• Super alloys (> 35 RC) : 80 – 140 m/min

• Hardened steels (> 45 RC): 100 – 300 m/min

In addition to speed, the most important factor that affects performance of CBN inserts is the preparation of cutting edge. It is best to use CBN tools with a honed or chamfered edge preparation, especially for interrupted cuts. Like ceramics, CBN tools are also available only in the form of index able inserts. The only limitation of it is its high cost.

(i) Diamond Tools

Single stone, natural or synthetic, diamond crystals are used as tips/edge of cutting tools. Owing to the extreme hardness and sharp edges, natural single crystal is used for many applications, particularly where high accuracy and precision are required. Their important uses are:

• Single point cutting tool tips and small drills for high speed machining of non-ferrous metals, ceramics, plastics, composites, etc. and effective machining of difficult-to-machine materials

• Drill bits for mining, oil exploration, etc.

• Tool for cutting and drilling in glasses, stones, ceramics, FRPs etc.

• Wire drawing and extrusion dies

• Super abrasive wheels for critical grinding.

Limited supply, increasing demand, high cost and easy cleavage of natural diamond demanded a more reliable source of diamond. It led to the invention and manufacture of artificial diamond grits by ultra-high temperature and pressure synthesis process, which enables large scale manufacture of diamond with some control over size, shape and friability of the diamond grits as desired for various applications.

Polycrystalline Diamond (PCD)

The polycrystalline diamond (PCD) tools consist of a layer (0.5 to 1.5 mm) of fine grain size, randomly oriented diamond particles sintered with a suitable binder (usually cobalt) and then metallurgically bonded to a suitable substrate like cemented carbide or Si3N4inserts. PCD exhibits excellent wear resistance, hold sharp edge, generates little friction in the cut, provide high fracture strength, and had good thermal conductivity. These properties contribute to PCD tooling's long life unconventional and high speed machining of soft, non-ferrous materials (aluminum, magnesium, copper etc), advanced composites and metal-matrix composites, super alloys, and non-metallic materials. PCD is particularly well suited for abrasive materials (i.e. drilling and reaming metal matrix composites) where it provides 100 times the life of carbides. PCD is not usually recommended for ferrous metals because of high solubility of diamond (carbon) in these materials at elevated temperature.

However, they can be used to machine some of these materials under special conditions; for example, light cuts are being successfully made in grey cast iron. The main advantage of such PCD tool is the greater toughness due to finer microstructure with random orientation of the grains and reduced cleavage. But such unique PCD also suffers from some limitations like:

• High tool cost

• Presence of binder, cobalt, which reduces wear resistance and thermal stability

• Complex tool shapes like in-built chip breaker cannot be made

• Size restriction, particularly in making very small diameter tools

The above mentioned limitations of polycrystalline diamond tools have been almost overcome by developing Diamond coated tools.

Diamond coated carbide tools

Since the invention of low pressure synthesis of diamond from gaseous phase, continuous effort has been made to use thin film diamond in cutting tool field. These are normally used as thin (<50 μm) or thick (> 200 μm) films of diamond synthesized by CVD method for cutting tools, dies, wear surfaces and even abrasives for Abrasive Jet Machining (AJM) and grinding. Thin film is directly deposited on the tool surface. Thick film (> 500 μm) is grown on an easy substrate and later brazed to the actual tool substrate and the primary substrate is removed by dissolving it or by other means. Thick film diamond finds application in making inserts, drills, reamers, end mills, routers. CVD coating has been more popular than single diamond crystal and PCD mainly for :

• Free from binder, higher hardness, and resistance to heat and wear more than PCD and properties close to natural diamond

• Highly pure, dense and free from single crystal cleavage

• Permits wider range of size and shape of tools and can be deposited on any shape of the tool including rotary tools

• Relatively less expensive

However, achieving improved and reliable performance of thin film CVD diamond coated tools; (carbide, nitride, ceramic, SiC etc) in terms of longer tool life, dimensional accuracy and surface finish of jobs essentially need:

1. Good bonding of the diamond layer

2. Adequate properties of the film, e.g. wear resistance, micro hardness, edge coverage, edge sharpness and thickness uniformity

3. Ability to provide work surface finish required for specific applications.

While CBN tools are feasible and viable for high speed machining of hard and strong steels and similar materials, Diamond tools are extremely useful for machining stones, slates, glass, ceramics, composites, FRPs and non ferrous metals specially which are sticky and BUE former such as pure aluminum and its alloys. CBN and Diamond tools are also essentially used for ultra precision as well as micro and nano machining.

MODULE-2

Cutting force components and their significances

The single point cutting tools being used for turning, shaping, planning, slotting, boring etc. are characterized by having only one cutting force during machining. But that force is resolved into two or three components for ease of analysis and exploitation. Fig. 2.1 visualizes how the single cutting force in turning is resolved into three components along the three orthogonal directions; X, Y and Z. The resolution of the force components in turning can be more conveniently understood from their display in 2-D as shown in Fig. 2.2.

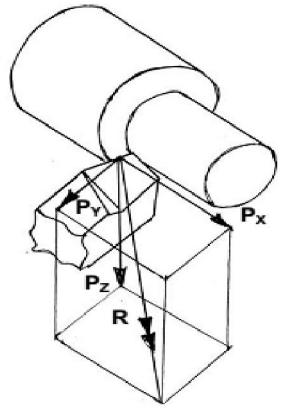

Fig.2.1Cutting force R resolved into P_X, P_Y and P_Z

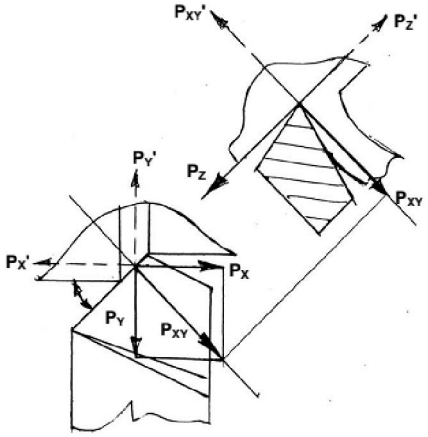

Fig. 2.2Turning force resolved into P_Z, P_X and P_Y

The resultant cutting force, R is resolved as,

$$\bar{R} = \bar{P}_z + \bar{P}_{xy} \quad (2.1)$$

$$\bar{P}_{xy} = \bar{P}_x + \bar{P}_y \quad (2.2)$$

Where, $P_X = P_{XY} \sin\varphi$ and $P_Y = P_{XY} \cos\varphi$ (2.3)

Where, P_Z= tangential component taken in the direction of Z_m axis

P_X= axial component taken in the direction of longitudinal feed or X_m axis

P_Y= radial or transverse component taken along Y_m axis.

In Fig. 2.1 and Fig.2.2 the force components are shown to be acting on the tool. A similar set of forces also act on the job at the cutting point but in opposite directions as indicated by P_Z', P_{XY}', P_X' and P_Y' in Fig.2. 2

Significance of P_Z, P_X and P_Y

P_Z: called the main or major component as it is the largest in magnitude. It is also called power component as it being acting along and being multiplied by V_C decides cutting power ($P_Z.V_C$) consumption.

P_y: may not be that large in magnitude but is responsible for causing dimensional inaccuracy and vibration.

P_X: It, even if larger than P_Y, is least harmful and hence least significant

Cutting forces in drilling

In a drill there are two main cutting edges and a small chisel edge at the centre as shown in Fig. 2.3. The force components that develop (Fig. 2.3) during drilling operation are:

• A pair of tangential forces, P_{T1} and P_{T2} (equivalent to P_Z in turning) at the main cutting edges

• Axial forces $P_{X1}$and P_{X2}acting in the same direction

• A pair of identical radial force components, $P_{Y1}$and P_{Y2}

• One additional axial force, P_{Xe} at the chisel edge which also removes material at the centre and under more stringent condition.

$P_{T1}$and P_{T2} produces the torque, T and causes power consumption P_C as,

$T = P_T x \frac{1}{2} (D)$ (2.4)

And $P_C = 2\pi TN$ (2.5)

Where, D = diameter of the drill

And N = speed of the drill in rpm.

The total axial force P_{XT} which is normally very large in drilling, is provided by

$$P_{XT} = P_{X1} + P_{X2} + P_{Xe} \quad (2.6)$$

But there is no radial or transverse force as PY1and PY2, being in opposite direction, nullify each other if the tool geometry is perfectly symmetrical.

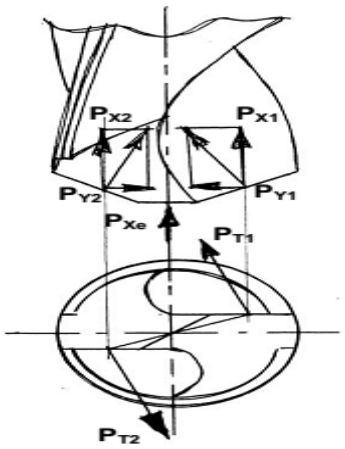

Fig. 2.3 Cutting forces in drilling.

Cutting forces in milling

The cutting forces (components) developed in milling with straight fluted slab milling cutter under single tooth engagement are shown in Fig. 2.4.

The forces provided by a single tooth at its angular position, ψ_I are:

•Tangential force P_{Ti} (equivalent to P_Z in turning)

• Radial or transverse force, P_{Ri} (equivalent to P_{XY} in turning)

• R is the resultant of P_T and P_R

• R is again resolved into P_Z and P_Y as indicated in Fig. 2.4 when Z and Y are the major axes of the milling machine.

Those forces have the following significance:

P_T governs the torque, T on the cutter or the milling arbour as

$T = P_T x\ D/2$ (2.7)

And also the power consumption, P_C as

$P_C = 2\pi TN$ (2.8)

Where, N = rpm of the cutter.

The other forces, P_R, P_Z, P_Y etc are useful for design of the

Machine – Fixture – Tool system.

In case of multi tooth engagement;

Total torque will be $D/2.\sum P_{Ti}$ and total force in Z and Y direction will be $\sum P_Z$ and $\sum P_Y$ respectively.

One additional force i.e. axial force will also develop while milling by helical fluted cutter

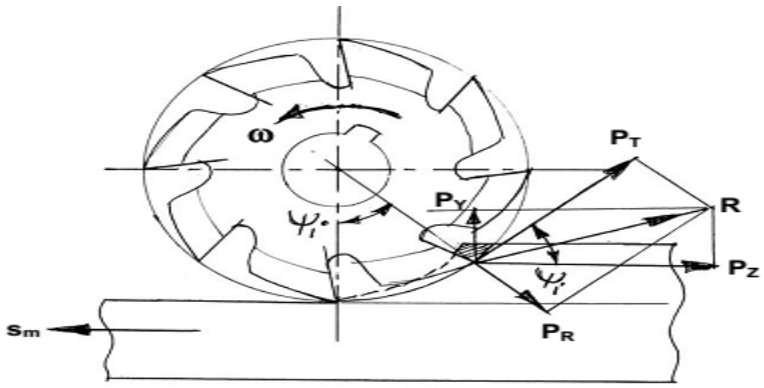

Fig. 2.4Cutting forces developed in plain milling

(With single tooth engagement)

Merchant's Circle Diagram and its use

In orthogonal cutting when the chip flows along the orthogonal plane, π_O, the cutting force (resultant) and its components PZ and PXY remain in the orthogonal plane. Fig. 2.5 is schematically showing the forces acting on a piece of continuous chip coming out from the shear zone at a constant speed. That chip is apparently in a state of equilibrium.

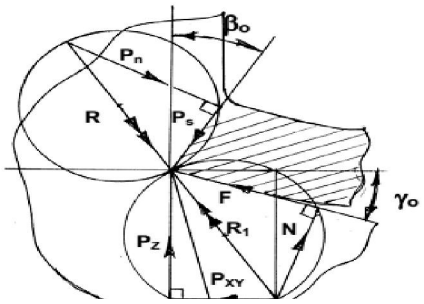

Fig. 2.5Development of Merchants Circle Diagram.

The forces in the chip segment are:

From job-side:

•P_S– shear force

•P_n– force normal to the shear force

Where, $\bar{P}_s + \bar{P}_n = \bar{R}$

From tool side:

$\bar{R}_1 = \bar{R}$ (in state of equilibrium)

Where, $\bar{R}_1 = \bar{F} + \bar{N}$

N = force normal to rake face.

•F = friction force at chip tool interface

The resulting cutting force R or R_1 can be resolved further as

$\bar{R}_1 = \bar{P}_z + \bar{P}_{xy}$

Where, P_Z= force along the velocity vector and P_{XY}= force along orthogonal plane.

The circle(s) drawn taking R or R_1 as diameter is called Merchant's circle which contains all the force components concerned as intercepts. The two circles with their forces are combined into one circle having all the forces contained in that as shown by the diagram called Merchant's Circle Diagram (MCD) in Fig. 2.6

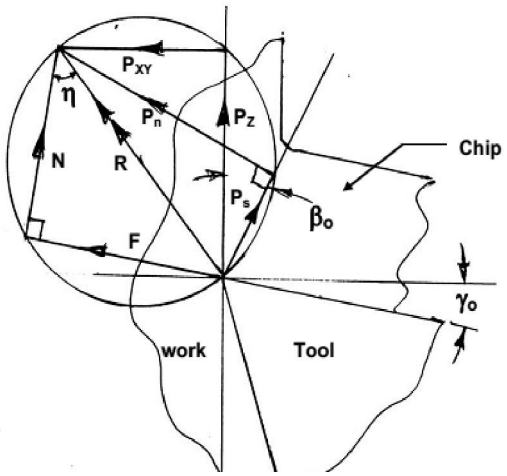

Fig. 2.6Merchant's Circle Diagram with cutting forces.

The significance of the forces displayed in the Merchant's Circle Diagram is:

P_S– the shear force essentially required to produce or separate the chip from the parent body by shear

P_n– inherently exists along with P_S

F – Friction force at the chip tool interface

N – Force acting normal to the rake surface

P_Z– main force or power component acting in the direction of cutting velocity

$\bar{P}_{xy} = \bar{P}_x + \bar{P}_y$

The magnitude of P_S provides the yield shear strength of the work material under the cutting condition.

The values of F and the ratio of F and N indicate interaction like friction at the chip-tool interface. The force components P_X, P_Y, P_Z are generally obtained by direct measurement. Again P_Z helps in determining cutting power and specific energy requirement. The force components are also required to design the cutting tool and the machine tool.

Advantages of using Merchant Circle Diagram (MCD)

Proper use of MCD enables the followings:

• Easy, quick and reasonably accurate determination several other forces from a few known forces involved in machining

• Friction at chip-tool interface and dynamic yield shear strength can be easily determined

• Equation relating to different forces can be easily developed

Some limitations of use of MCD

- Merchant's Circle Diagram (MCD) is valid only for orthogonal cutting
- By the ratio, F/N, the MCD gives apparent (not actual) coefficient of friction
- It is based on single shear plane theory.

The advantages of constructing and using MCD has been illustrated as by an example as follows

Suppose, in a simple straight turning under orthogonal cutting condition with given speed, feed, depth of cut and tool geometry, the only two force components P_Z and P_X are known by experiment i.e., direct measurement, then how can one determine the other relevant forces and machining characteristics easily and quickly without going into much equations and calculations but simply constructing a circle-diagram.

This can be done by taking the following sequential steps

- Determine P_{XY} from $P_X = P_{XY} \sin\varphi$ and $P_Y = P_{XY} \cos\varphi$
- Draw the tool and the chip in orthogonal plane with the given value of γ_o as shown in Fig. 2.6
- Choose a suitable scale (e.g. 100 N = 1 cm) for presenting P_Z and P_{xy} in cms
- Draw P_z & P_{xy} along and normal to V_C as indicated in fig 2.6
- Draw the cutting force R as the resultant of P_Z and P_{XY}
- Draw the circle (Merchant's circle) taking R as diameter
- Get F and N as intercepts in the circle by extending the tool rake surface and joining tips of F and R
- Divide the intercepts of F and N by the scale and get the values of F and N
- For determining P_s (and P_n) the value of the shear angle β_o has to be evaluated from $tan\beta_0 = \frac{cos\gamma_0}{\zeta - \sin\gamma_0}$ Where γ_0 is known and ζ has to be obtained from $\zeta = \frac{a_2}{a_1}$ where $a_1 = s_0 \sin\varphi$
- s_o and φ are known and a_2 is either known , if not, it has to be measured by micrometer or slide caliper
- Draw the shear plane with the value of β_0 and then P_s and P_n as intercepts shown in Fig. 2.6.
- Get the values of P_s and P_n by dividing their corresponding lengths by the scale

- Get the value of apparent coefficient of friction, μ_a at the chip tool interface simply from the ratio,$\mu_a = \frac{F}{N}$
- Get the friction angle, η, if desired, either from tanη= μ_a or directly from the MCD drawn as indicated in Fig. 2.6
- Determine dynamic yield shear strength (τ_s) of the work material under the cutting condition using the simple expression $\tau_s = \frac{P_s}{A_s}$ where, A_s= shear area as indicated in Fig. 2.7
  $= \frac{a_1 b_1}{sin\beta_0} = \frac{ts_0}{sin\beta_0}$, t = depth of cut (known)

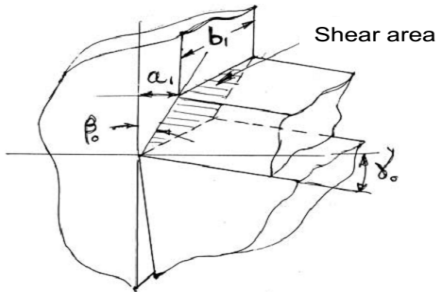

Fig.2.7 Shear area in orthogonal turning

Energy of cutting process

Total energy per unit volume of metal removed =$U_c = \frac{P_z V}{A_0 V}$

Where $A_0 = a_1 b_1$

V=velocity of cutting

Total energy per unit volume is consumed in the following way

a) Shear energy per unit volume(U_s)
b) Specific friction energy(U_f)
c) Surface energy per unit volume(U_A)
d) Momentum energy per unit volume(U_m)

The Surface energy per unit volume and Momentum energy per unit volume are negligible relative to other components and can be disregarded in calculation,

The Shear energy per unit volume is obtained from,

$$U_s = \frac{P_s V_s}{A_0 V_c} = \frac{P_s V_s}{\sin\beta\ V} = \frac{\zeta_s}{\sin\beta} \frac{V cos\gamma_0}{V cos(\beta - \gamma_0)} = \zeta_s \varepsilon$$

The Specific friction energy is given by,

$$U_F = \frac{F.V_c}{A_0.V} = \frac{F.V.r}{a_1 b_1 V} = \frac{F}{\zeta a_1 b_1}$$

As energy balance can be established by taking velocity relationship into account

$$U_c = \frac{P_z V}{A_0 V} = \frac{P_z}{A_0} = \frac{P_z}{A_0}\frac{cos(\beta-\gamma_0)}{cos(\beta-\gamma_0)} = \frac{P_z}{A_0}\left[\frac{cos\beta cos\gamma_0 + \sin\beta sin\gamma_0}{cos(\beta-\gamma_0)}\right]$$

$$= \frac{R}{A_0}\left[\frac{cos(\eta-\gamma_0)cos\beta cos\gamma_0 + cos(\eta-\gamma_0)\sin\beta sin\gamma_0}{cos(\beta-\gamma_0)}\right]$$

$$= \frac{R}{A_0}\left[\frac{cos\eta\ cos\gamma_0\ cos\beta\ cos\gamma_0 + sin\eta\ sin\gamma_0\ cos\beta\ cos\gamma_0 + cos\eta\ cos\gamma_0 \sin\beta sin\gamma_0 + cos\eta\ cos\gamma_0 \sin\beta sin\gamma_0}{cos(\beta-\gamma_0)}\right]$$

$$= \frac{R}{A_0}\left[\frac{\cos(\eta+\beta-\gamma_0)\ cos\gamma_0 + \sin(\eta-\gamma_0)\ sin\beta\ cos\gamma_0 + \cos(\eta-\gamma_0)\sin\beta sin\gamma_0}{cos(\beta-\gamma_0)}\right]$$

$$= \frac{P_s}{A_0}\frac{cos\gamma_0}{cos(\beta-\gamma_0)} + \frac{Rsin\beta}{A_0 cos(\beta-\gamma_0)}[\sin(\eta-\gamma_0)\ cos\gamma_0 + \cos(\eta-\gamma_0)\ cos\gamma_0]$$

$$= \frac{P_s}{A_0}\frac{cos\gamma_0}{sin\beta cos(\beta-\gamma_0)} + \frac{\frac{P_z}{\cos(\eta-\gamma_0)}sin\beta}{A_0 cos(\beta-\gamma_0)}[\sin(\eta-\gamma_0)\ cos\gamma_0 + \cos(\eta-\gamma_0)\ cos\gamma_0]$$

$$= \zeta_s\varepsilon + \frac{sin\beta}{A_0 cos(\beta-\gamma_0)}[P_z\tan(\eta-\gamma_0)\ cos\gamma_0 + P_z sin\gamma_0]$$

For orthogonal turning φ=90^0

$$= \zeta_s\varepsilon + \frac{sin\beta}{A_0 cos(\beta-\gamma_0)}\left[P_{xy}cos\gamma_0 + P_z sin\gamma_0\right]$$

$$= \zeta_s\varepsilon + \frac{F}{A_0\zeta} \Rightarrow U_c = U_s + U_f$$

Practically all the energy required in metal cutting is consumed in the plastic deformation on the shear plane and for overcoming the friction between the chip and tool.

$$U_s = U_c - U_f \Rightarrow \zeta_s\varepsilon = \frac{P_z}{a_1 b_1} - \frac{F}{\zeta a_1 b_1} = \frac{P_z}{a_1 b_1}\left(1 - \frac{F}{\frac{P_z}{\zeta}}\right) = \frac{P_z}{a_1 b_1}\left(1 - \frac{sin\eta}{\zeta\cos(\eta-\gamma_0)}\right)$$

$$\Rightarrow P_z = \frac{\zeta_s \varepsilon a_1 b_1}{\left(1 - \frac{sin\eta}{\zeta \cos(\eta - \gamma_0)}\right)}$$

This expression indicates the dependency of P_z on the values of ζ_s, ζ and cutting parameters a_1, b_1

Velocities in metal cutting

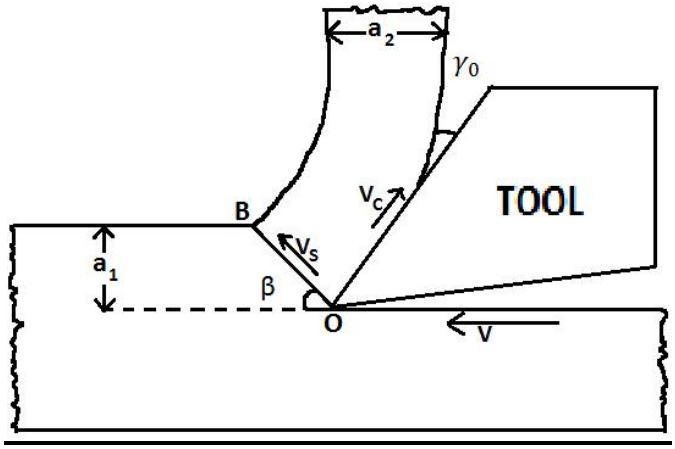

1. Cutting velocity (V): it is the velocity of cutting tool relative to the work piece and directed parallel to cutting force.
2. Chip velocity (V_c): it is the velocity of the chip relative to the tool and is directed along the tool face.
3. Shear velocity(V_s):it is the velocity of the chip relative to the work piece and directed along the shear plane

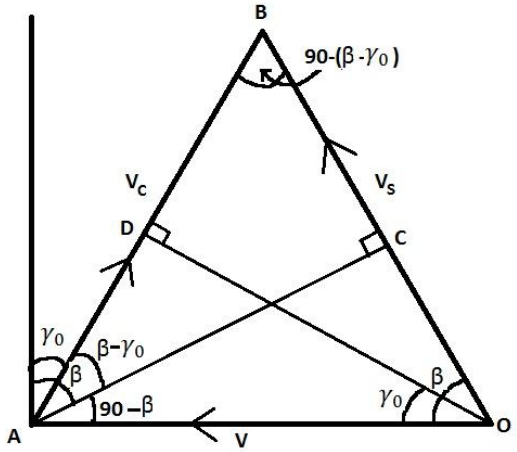

Let V_c = directed along the tool face
V_s = directed along the shear plane
V = directed along the cutting force
a_1 = chip thickness before cut

$a_2 = chip\ thickness\ after\ cut$

$r = chip\ thickness\ ratio = \frac{a_1}{a_2}$

$\zeta = \frac{a_2}{a_1} = \frac{1}{r} = \frac{\cos(\beta - \gamma_0)}{sin\beta} = chip\ reduction\ co-efficient$

$\beta = shear\ angle$

From right angle triangle ΔOCA,

$$sin\beta = \frac{AC}{OA} \Rightarrow AC = OA\ sin\beta \Rightarrow AC = Vsin\beta \quad (1)$$

From right angle triangle ΔBAC,

$$\cos(\beta - \gamma_0) = \frac{AC}{AB} \Rightarrow AC = AB\cos(\beta - \gamma_0) \Rightarrow AC = V_C\cos(\beta - \gamma_0) \quad (2)$$

From equation (1) and (2)

$$Vsin\beta = V_C\cos(\beta - \gamma_0) \Rightarrow V_C = \frac{Vsin\beta}{\cos(\beta - \gamma_0)} = V.r$$

From right angle triangle ΔODA,

$$cos\gamma_0 = \frac{OD}{OA} \Rightarrow OD = OAcos\gamma_0 \Rightarrow OD = Vcos\gamma_0 \quad (3)$$

From right angle triangle ΔODB,

$$\cos(\beta - \gamma_0) = \frac{OD}{OB} \Rightarrow OD = OB\cos(\beta - \gamma_0) \Rightarrow OD = V_s\cos(\beta - \gamma_0) \quad (4)$$

From equation (3) and (4)

$$Vcos\gamma_0 = V_s\cos(\beta - \gamma_0) \Rightarrow V_s = \frac{Vcos\gamma_0}{V_s\cos(\beta - \gamma_0)}$$

Theoretical determination of cutting forces

The tangential cutting force for orthogonal rake system is

$$P_z = \frac{\zeta_s a_1 b_1 \cos(\eta - \gamma_0)}{\cos(\eta + \beta - \gamma_0)\ sin\beta}$$

Where, s=feed, mm/rev
t =depth of cut, mm
ζ_s=dynamic shear stress, kg/mm^2
η=friction angle
γ_0=orthogonal rake angle

β=shear angle

The known parameters are

1. the cutting area=$a_1 b_1 = st$
2. the rake angle=γ_0

The problems involved in the determination of cutting forces are

1. The problem of determining ζ_s under cutting condition.
2. The problem of finding out suitable angle relationship for evaluating $(\eta + \beta - \gamma_0)$

Ernst and merchant's relationship

Assumption

1. The shear stress is a true property of work material i.e. ζ_s=k
2. The total energy input to the system has been consumed in deformation.
$$\frac{dW}{dt} = P_z V_c$$
3. The friction process at the chip tool interface is invariant i.e. $\eta = constant$

Total energy input to the system is

$$E = \frac{dW}{dt} = P_z V_c = \frac{k a_1 b_1 \cos(\eta - \gamma_0) V_c}{\cos(\eta + \beta - \gamma_0)\, sin\beta}$$

By applying principle of minimum energy

$$\frac{dP_z}{d\beta} = -k a_1 b_1 \cos(\eta - \gamma_0)\left[\frac{\cos\beta \,.\cos(\eta + \beta - \gamma_0) - \sin\beta \,.\sin(\eta + \beta - \gamma_0)}{sin^2\beta . cos^2(\eta + \beta - \gamma_0)}\right] = 0$$

$\Rightarrow \cos\beta \,.\cos(\eta + \beta - \gamma_0) - \sin\beta \,.\sin(\eta + \beta - \gamma_0) = 0$

$\Rightarrow \cos(\beta + \beta + \eta - \gamma_0) = 0$

$\Rightarrow 2\beta + \eta - \gamma_0 = \frac{\pi}{2}$

Limitation

1. Non compatibility with the actual deformation process
2. The non cognizance of the dependency of $\beta \; and \; \eta$

Lee-Shaffer's Relationship

Assumption

1. The material in the stress field is ideally plastic and non hardening
2. The shear plane coincides with the direction of maximum shear stress

Based on the following assumption they derived the following relationship

$$\beta + \eta - \gamma_0 = \frac{\pi}{4}$$

Evaluation of cutting power consumption and specific energy requirement

Cutting power consumption is a quite important issue and it should always be tried to be reduced but without sacrificing MRR.

Cutting power consumption, P_C can be determined from,

$P_c = P_z V_c + P_x V_f$

Where, V_f= feed velocity=$\frac{Ns_0}{1000} m/min$ [N=r.p.m]

Since both P_X and V_f, specially V_f are very small, $P_X.V_f$ can be neglected and then $P_C \cong P_Z.V_C$

Specific energy requirement, which means amount of energy required to remove unit volume of material, is an important machinability characteristics of the work material. Specific energy requirement, U_s, which should be tried to be reduced as far as possible, depends not only on the work material but also the process of the machining, such as turning, drilling, grinding etc. and the machining condition, i.e., V_C, so, tool material and geometry and cutting fluid application.

Compared to turning, drilling requires higher specific energy for the same work-tool materials and grinding requires very large amount of specific energy for adverse cutting edge geometry (large negative rake). Specific energy, U_s is determined from $U_s = \frac{P_z V_c}{MRR} = \frac{P_z}{ts_0}$

Development of mathematical expressions for cutting forces under orthogonal turning.

• Tangential or main component, P_z

This can be very conveniently done by using Merchant's Circle Diagram, MCD, as shown in Fig. 2.8

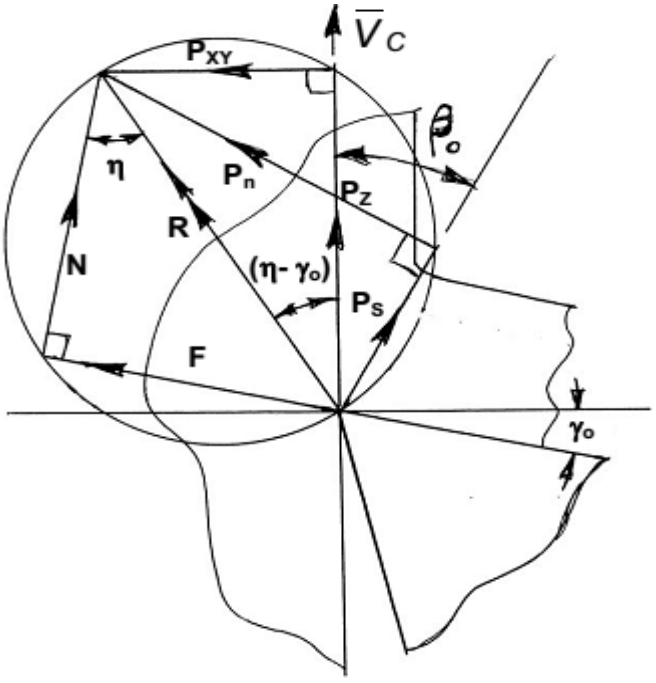

Fig. 2.8 Forces involved in machining and contained in Merchant's Circle.

From the diagram in Fig. 2.8,

$$P_Z = Rcos(\eta - \gamma_0) \quad (2.9)$$

$$P_s = Rcos(\beta_0 + \eta - \gamma_0) \quad (2.10)$$

Dividing Eqn. 2.9 by Eqn. 2.10,

$$P_Z = \frac{P_s cos(\eta - \gamma_0)}{cos(\beta_0 + \eta - \gamma_0)} \quad (2.11)$$

It was already shown that,

$$P_s = \frac{tS_0\tau_s}{sin\beta_0} \quad (2.12)$$

Where, τ_s = dynamic yield shear strength of the work material.

Thus, $P_Z = \frac{tS_0\tau_s\, cos(\eta - \gamma_0)}{sin\beta_0 cos(\beta_0 + \eta - \gamma_0)}$ (2.13)

For brittle work materials, like grey cast iron, usually, $2\beta_0 + \eta - \gamma_0 = 90^0$ and τ_s remains almost unchanged.

Then for turning brittle material,

$$P_Z = \frac{tS_0\tau_s cos(90^0 - 2\beta_0)}{sin\beta_0 cos(90^0 - \beta_0)}$$

Or, $P_Z = 2tS_0\tau_s cot\beta_0$ (2.14)

Where, $cot\beta_0 = \zeta - tan\gamma_0$ (2.15)

$\zeta = \frac{a_2}{a_1} = \frac{a_2}{S_0 sin\theta}$

It is difficult to measure chip thickness and evaluate the values of ζ while machining brittle materials and the value of τ_s is roughly estimated from

$$\tau_s = 0.175BHN \quad (2.16)$$

Where, BHN = Brinnel Hardness number.

But most of the engineering materials are ductile in nature and even some semi-brittle materials behave ductile under the cutting condition.

The angle relationship reasonably accurately applicable for ductile metals is

$$\beta_0 + \eta - \gamma_0 = 45^0 \quad (2.17)$$

And the value of τ_s is obtained from,

$$\tau_s = 0.186\ BHN \text{ (Approximate)} \quad (2.18)$$

$$\text{Or} = 0.74\sigma_u\varepsilon^{0.6\Delta} \text{ (more suitable and accurate)} \quad (2.19)$$

Where, σ_u= ultimate tensile strength of the work material

ε= cutting strain

$\cong \zeta - tan\gamma_0$

And Δ= $\%\ elongation$

Substituting Eqn. 2.17 in Eqn. 2.13,

$$P_Z = tS_0\tau_s(cot\beta_0 + 1) \quad (2.20)$$

Again $cot\beta_0 \cong \zeta - tan\gamma_0$

So, $P_Z = tS_0\tau_s(\zeta - tan\gamma_0 + 1)$ (2.21)

- **Axial force, P_X and transverse force, P_Y**

From MCD in Fig. 2.8,

$$P_{XY} = P_Z tan(\eta - \gamma_0) \quad (2.22)$$

Combining Eqn. 9.5 and Eqn. 9.14,

$$P_{XY} = \frac{tS_0\tau_s sin(\eta-\gamma_0)}{sin\beta_0 cos(\beta_0+\eta-\gamma_0)} \quad (2.23)$$

Again, using the angle relationship$\beta_0 + \eta - \gamma_0 = 45^0$, for ductile material

$$P_{XY} = tS_0\tau_s(cot\beta_0 - 1) \quad (2.24)$$

Or $P_{XY} = tS_0\tau_s(\zeta - tan\gamma_0 - 1)$ (2.25)

Where, $\tau_s = 0.74\sigma_u\varepsilon^{0.6\Delta}$ or 0.186 BHN

It is already known,

$$P_X = P_{XY} sin\theta$$

And $P_Y = P_{XY} cos\theta$

Therefore, $P_X = tS_0\tau_s(\zeta - tan\gamma_0 - 1)\ sin\theta$ (2.26)

And $P_Y = tS_0\tau_s(\zeta - tan\gamma_0 - 1)\ cos\theta$ (2.27)

• Friction force, F, normal force, N and apparent coefficient of friction μ_a

Again from the MCD in Fig. 2.8

$$F = P_Z sin\gamma_0 + P_{XY} cos\gamma_0 \quad (2.28)$$

And $N = P_Z cos\gamma_0 - P_{XY} sin\gamma_0$ (2.29)

And $\mu_a = \frac{F}{N} = \frac{P_Z sin\gamma_0 + P_{XY} cos\gamma_0}{P_Z cos\gamma_0 - P_{XY} sin\gamma_0}$ (2.30)

Or, $\mu_a = \frac{P_Z tan\gamma_0 + P_{XY}}{P_Z - P_{XY} tan\gamma_0}$ (2.31)

Therefore, if P_Z and P_{XY} are known or determined either analytically or experimentally the values of F, N and μ_a can be determined using equations only.

• Shear force P_s and P_n

Again from the MCD in Fig. 2.8

$$P_s = P_Z cos\beta_0 - P_{XY} sin\beta_0 \quad (2.32)$$

And $P_n = P_Z sin\beta_0 + P_{XY}\ cos\beta_0$ (2.33)

FromP_s, the dynamic yield shear strength of the work material, τ_s can be determined by using the relation,

$$P_s = A_s\tau_s$$

Where, $A_s = shear\ area = \frac{tS_0}{sin\beta}$

Therefore, $\tau_s = \frac{P_s sin\beta_0}{tS_0}$

$$= \frac{(P_Z cos\beta_0 - P_{XY} sin\beta_0) sin\beta_0}{tS_0} \quad (2.34)$$

Dynamometers for measuring cutting forces

Different types of transducers used in dynamometers for measuring machining forces.

Measurement of cutting force(s) is based on three basic principles:

(a) Measurement of elastic deflection of a body subjected to the cutting force

(b) Measurement of elastic deformation, i.e. strain induced by the force

(c) Measurement of pressure developed in a medium by the force.

The type of the transducer depends upon how that deflection, strain or pressure is detected and quantified.

(a) Measuring deflection caused by the cutting force(s)

Under the action of the cutting force, say P_Z in turning, the tool or tool holder elastically deflects as indicated in Fig. 2.9. Such tool deflection, δ is proportional to the magnitude of the cutting force,P_Z, simply as,

$$\delta = P_Z \left(\frac{L^3}{3EI}\right) \tag{2.35}$$

Where, L = overhang or equivalent projected length of the cantilever type tool (holder)

E = physical property (Young's modulus of elasticity of the beam)

I = size (plane moment of inertia) of the beam section.

Since for a given cutting tool and its holder, E and I are fixed and the equation 2.35 becomes,

$$\delta \alpha P_Z \text{ or } \delta = kP_Z \tag{2.36}$$

Where, k is a constant of proportionality.

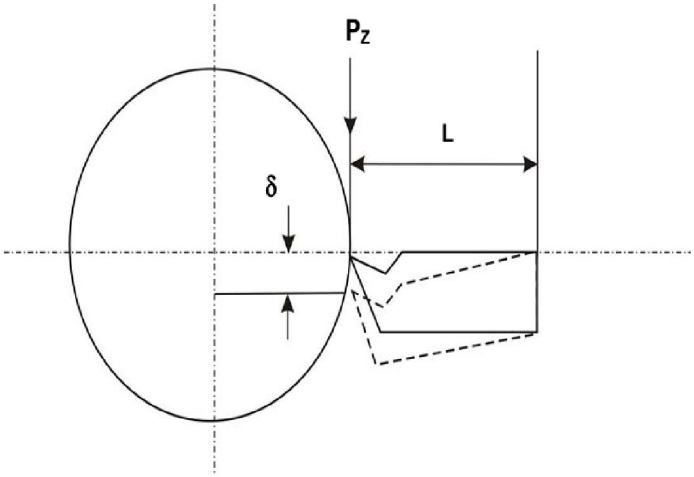

Fig. 2.9 Cutting tool undergoing deflection, δ due to cutting force,P_Z

The deflection, δ, can be measured

• Mechanically by dial gauge (mechanical transducer)

• Electrically by using several transducers like;

- – potentiometer; linear or circular
- –capacitive pickup
- –inductive pickup
- –LVDT

as schematically shown in Fig. 2.10.

• Opto-electronically by photocell where the length of the slit through which light passes to the photocell changes proportionally with the tool – deflection.

All such transducers need proper calibration before use.

In case of mechanical measurement of the tool deflection by dial gauge, calibration is done by employing known loads, W and the corresponding tool deflections, δ are noted and then plotted as shown in Fig. 2.11. Here the slope of the curve represents the constant, k of the equation 2.36. Then while actual measurement of the cutting force, PZ, the δ*is noted and the corresponding force is assessed from the plot as shown.

In capacitive pick up type dynamometer, the cutting force causes proportional tool deflection, δ, which causes change in the gap (d) and hence capacitance, C as $c = \frac{\varepsilon A}{3.6\pi d}$ (2.37)

The change in C is then measured in terms of voltage, ΔV which becomes proportional to the force. The final relation between P_Z and ΔV is established by calibration.

In case of LVDT, the linear movement of the core, (coupled with the tool), inside the fixed coil produces proportional voltage across the secondary coil.

Fig. 2.10 Electrical transducers working based on deflection measurement

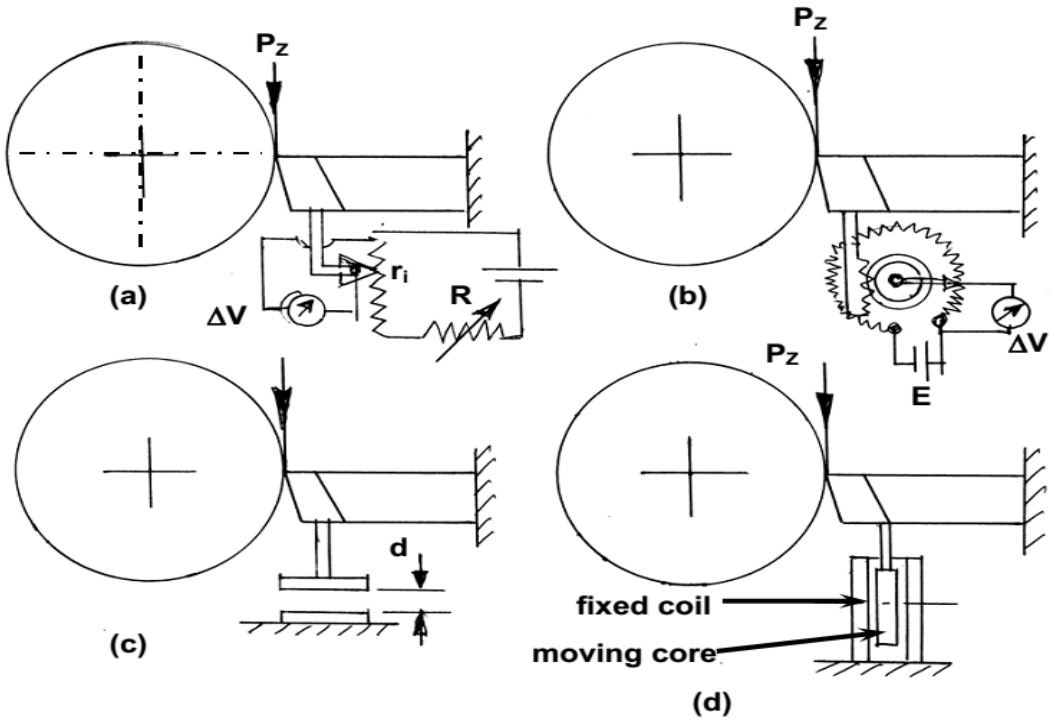

Fig. 2.10 Electrical transducers working based on deflection measurement

(a) linear pot (b) circular pot (c) capacitive pick up (d) LVDT type

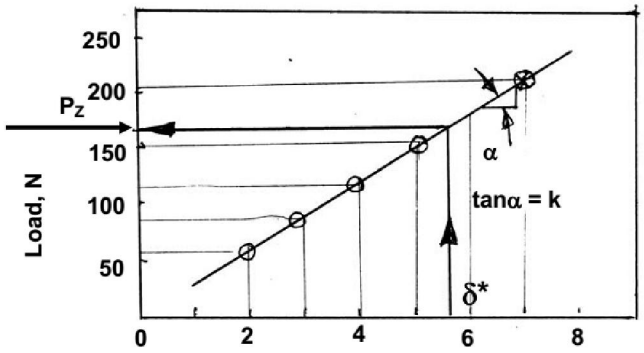

Fig. 2.11 Calibration of mechanical measurement system (dial gauge)

(b) Measuring cutting force by monitoring elastic strain caused by the force.

Increasing deflection, δ enhances sensitivity of the dynamometer but may affect machining accuracy where large value of δ is restricted; the cutting forces are suitably measured by using the change in strain caused by the force. Fig. 2.12 shows the principle of force measurement by measuring strain, ε, which would be proportional with the magnitude of the force, F (say P_Z) as,

$$\varepsilon = \frac{\sigma}{E} = \frac{M/Z}{E} = \frac{P_Z.l}{ZE} = k_1 P_Z \tag{2.38}$$

where, M = bending moment

Z = sectional modulus (I/y) of the tool section

I = plane moment of inertia of the plane section

y = distance of the straining surface from the neutral plane of the beam (tool)

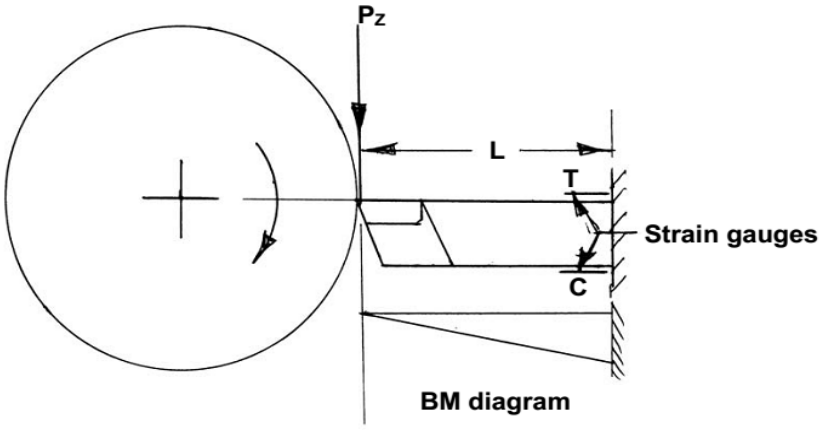

Fig. 2.12 Measuring cutting forces by strain gauges

The strain, ε induced by the force changes the electrical resistance, R, of the strain gauges which are firmly pasted on the surface of the tool-holding beam as

$$\frac{\Delta R}{R} = G\varepsilon \tag{2.39}$$

Where, G = gauge factor (around 2.0 for conductive gauges)

The change in resistance of the gauges connected in a Wheatstone bridge produces voltage output ΔV, through a strain measuring bridge (SMB) as indicated in Fig. 10.6.

Out of the four gauges, R_1, R_2, R_3 and R_4, two are put in tension and two in compression as shown in Fig. 2.13 The output voltage, ΔV, depends upon the constant, G and the summation of strains as,

$$\Delta V = \frac{GE}{4}[\varepsilon_1 - (-\varepsilon_2) + \varepsilon_3 - (-\varepsilon_4)]$$

(2.40)

Where, ε_1 and ε_2 are in tension and - ε_3 and - ε_4 are in compression

The gauge connections may be

- full bridge (all 4 gauges alive) – giving full sensitivity
- half bridge (only 2 gauges alive) – half sensitive
- quarter bridge (only 1 gauge alive) – ¼ th sensitivity

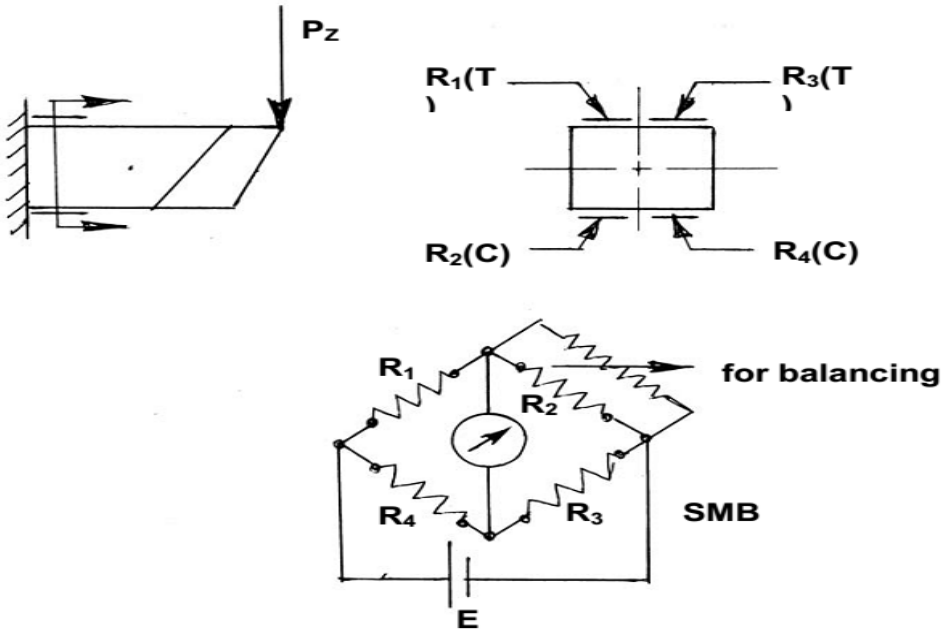

Fig. 2.13 Force measurement by strain gauge based transducer.

(c)Measuring cutting forces by pressure caused by the force

This type of transducer functions in two ways:

• The force creates hydraulic pressure (through a diaphragm or piston) which is monitored directly by pressure gauge

• the force causes pressure on a piezoelectric crystal and produces an emf proportional to the force or pressure as indicated in Fig. 2.14.

Here, $emf = \lambda tp$ (2.41)

where λ= voltage sensitivity of the crystal

t = thickness of the crystal

p = pressure

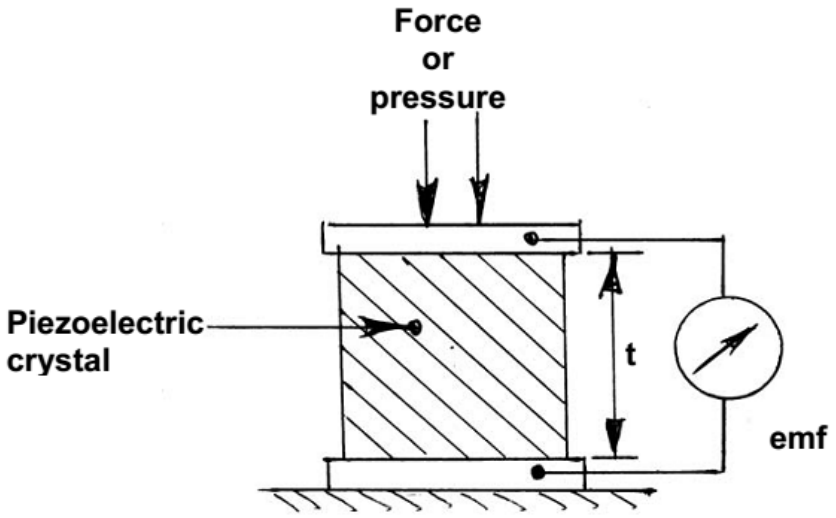

Fig. 2.14 Piezoelectric transducer for measuring force or pressure.

(iii) Design requirements for Tool – force Dynamometers

For consistently accurate and reliable measurement, the following requirements are considered during design and construction of any tool force dynamometers:

• **Sensitivity**: the dynamometer should be reasonably sensitive for precision measurement

• **Rigidity**: the dynamometer need to be quite rigid to withstand the forces without causing much deflection which may affect the machining condition

• **Cross sensitivity**: the dynamometer should be free from cross sensitivity such that one force (say P_Z) does not affect measurement of the other forces (say P_X and P_Y)

• Stability against humidity and temperature

•Quick time response

• High frequency response such that the readings are not affected by vibration within a reasonably high range of frequency

• Consistency, i.e. the dynamometer should work desirably over a long period.

(iv) Construction and working principle of some common tool – force dynamometers.

The dynamometers being commonly used now-a-days for measuring machining forces desirably accurately and precisely (both static and dynamic characteristics) are either strain gauge type or piezoelectric type

Strain gauge type dynamometers are inexpensive but less accurate and consistent, whereas, the piezoelectric type are highly accurate, reliable and consistent but very expensive for high material cost and stringent construction.

• Turning Dynamometer

Turning dynamometers may be strain gauge or piezoelectric type and may be of one, two or three dimensions capable to monitor all of P_X, P_Y and P_Z. For ease of manufacture and low cost, strain gauge type turning dynamometers are widely used and preferably of 2 – D (dimension) for simpler construction, lower cost and ability to provide almost all the desired force values.

Design and construction of a strain – gauge type 2 – D turning dynamometer are shown schematically in Fig. 2.15 and photographically in Fig. 2.16 Two full bridges comprising four live strain gauges are provided for P_Z and P_X channels which are connected with the strain measuring bridge for detection and measurement of strain in terms of voltage which provides the magnitude of the cutting forces through calibration. Fig. 2.17 pictorially shows use of 3 – D turning dynamometer having piezoelectric transducers inside.

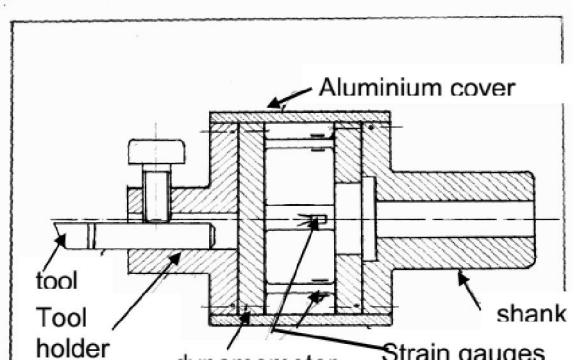

Fig. 2.15 Schematic view of a strain gauge type 2 – D turning dynamometer.

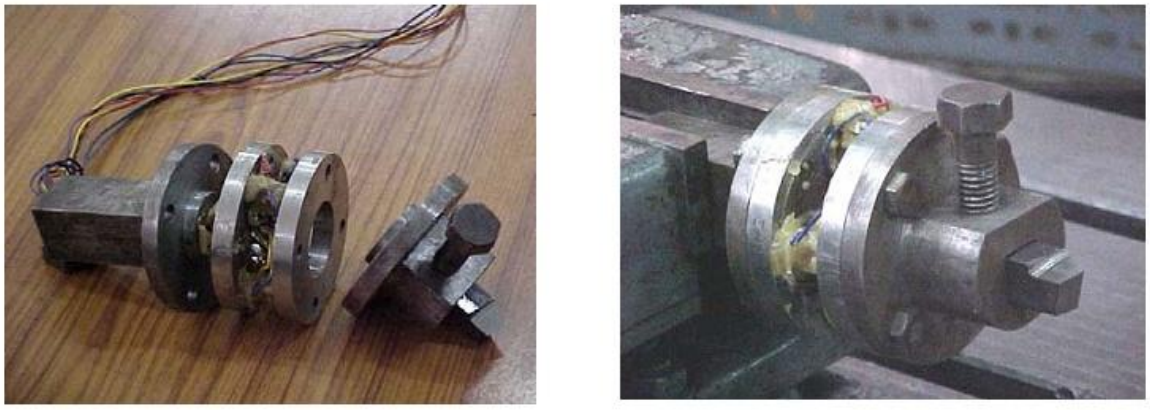

Fig. 2.16 Photographs of a strain gauge type 2 – D turning dynamometer and its major components.

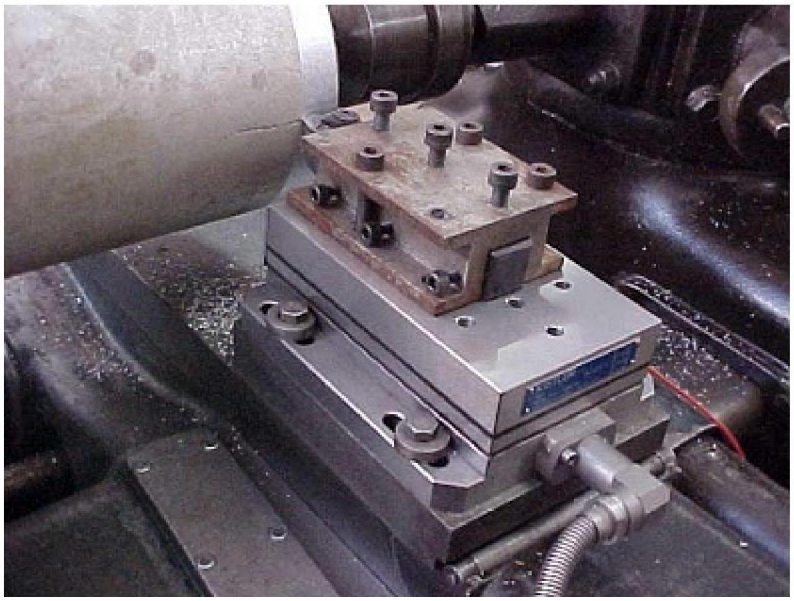

Fig. 2.17 Use of 3 – D piezoelectric type turning dynamometer.

• Drilling dynamometer

Physical construction of a strain gauge type 2 – D drilling dynamometer for measuring torque and thrust force is typically shown schematically in Fig. 2.18 and pictorially in Fig. 2.19. Four strain gauges are mounted on the upper and lower surfaces of the two opposite ribs for PX– channel and four on the side surfaces of the other two ribs for the torque channel. Before use, the dynamometer must be calibrated to enable determination of the actual values of T and P_X from the voltage values or reading taken in SMB or PC.

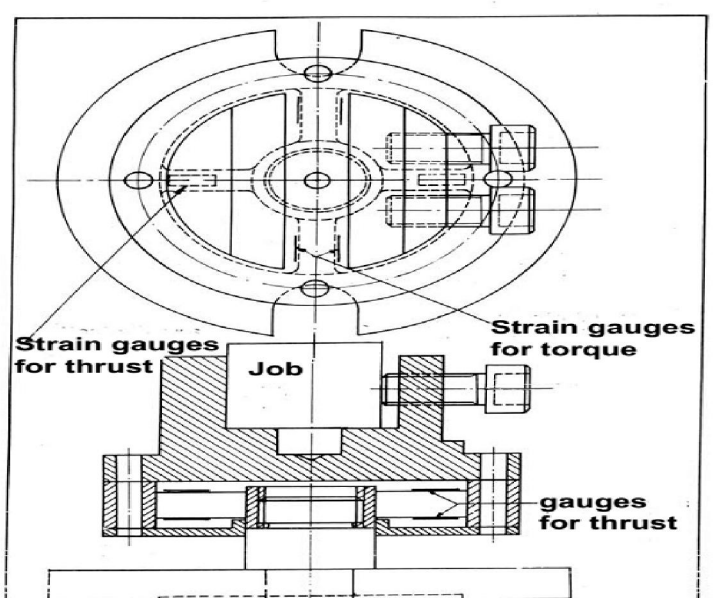

Fig. 2.18 Schematic view of construction of a strain gauge type drilling dynamometer.

Fig. 2.19 A strain gauge type drilling dynamometer and its major components.

• Milling dynamometer

Since the cutting or loading point is not fixed w.r.t. the job and the dynamometer, the job platform rests on four symmetrically located supports in the form of four O-rings. The forces on each O-ring are monitored and summed up correspondingly for getting the total magnitude of all the three forces in X, Y and Z direction respectively.

Fig. 2.20 shows schematically the principle of using O-ring for measuring two forces by mounting strain gauges, 4 for radial force and 4 for transverse force

.

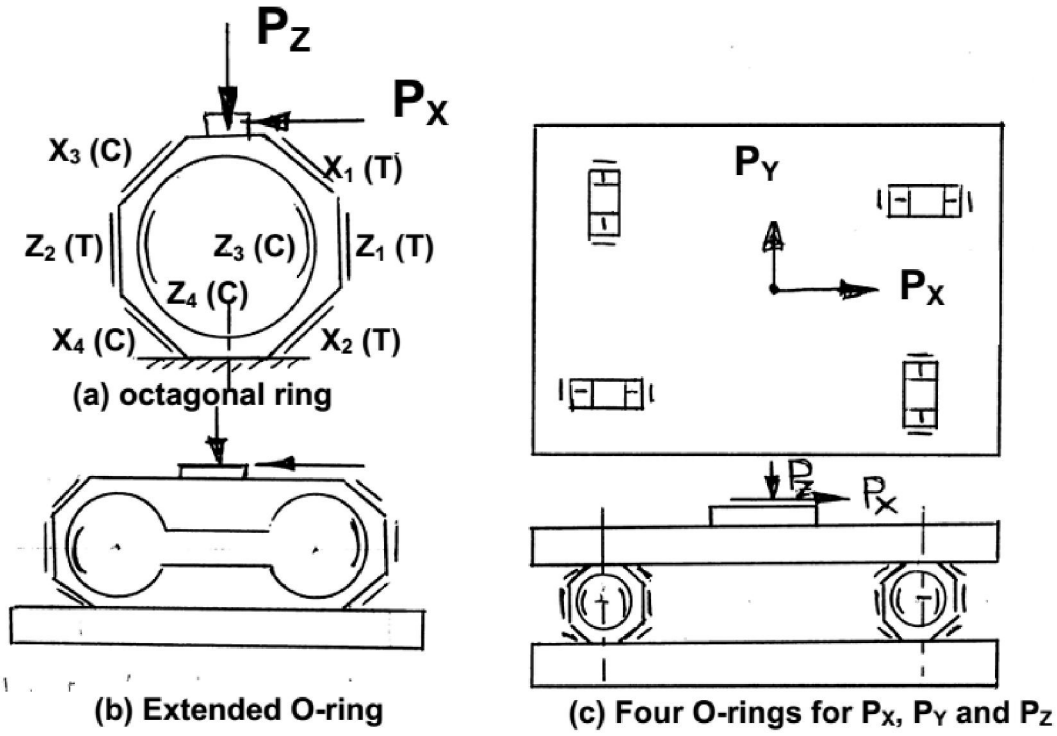

Fig. 2.20 Scheme of strain gauge type 3 – D milling dynamometer

Fig. 2.21 typically shows configuration of a strain gauge type 3 – D milling dynamometer having 4 octagonal rings. Piezoelectric type 3 – D dynamometers are also available and used for measuring the cutting forces in milling (plain, end and face)

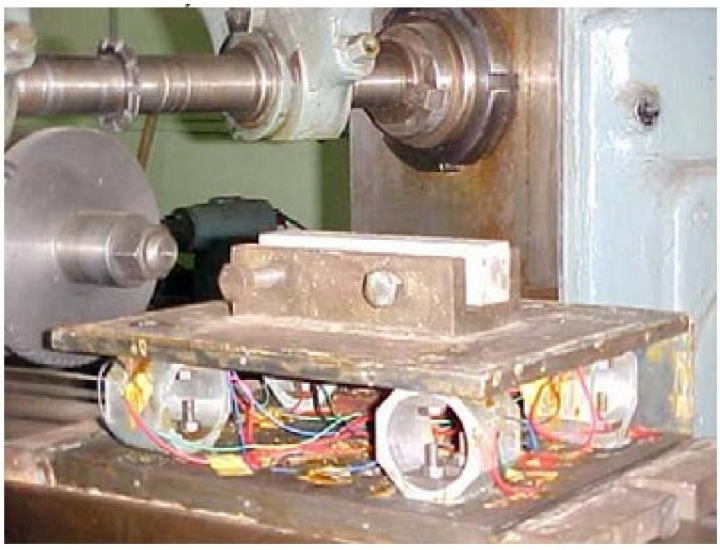

Fig. 2.21 A typical strain gauge type 3 – D milling dynamometer

MODULE-3

Cutting temperature – causes, effects, assessment and control

Determine the value of cutting temperature.

- •Analytical methods
- •Experimental methods

Sources and causes of heat generation and development of temperature in machining

During machining heat is generated at the cutting point from three sources, as indicated in Fig. 3.1. Those sources and causes of development of cutting temperature are:

- Primary shear zone (1) where the major part of the energy is converted into heat
- Secondary deformation zone (2) at the chip – tool interface where further heat is generated due to rubbing and / or shear
- At the worn out flanks (3) due to rubbing between the tool and the finished surfaces.

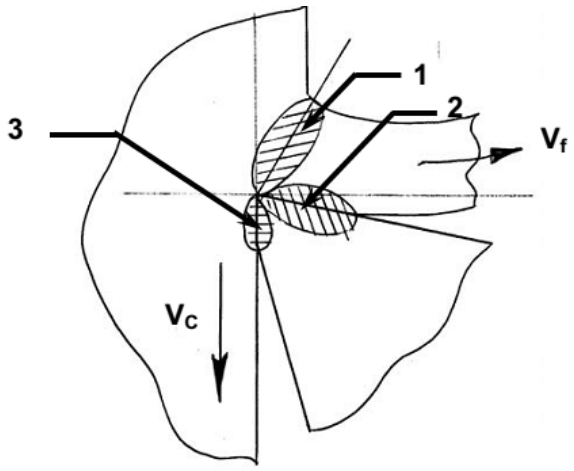

Fig. 3.1 Sources of heat generation in machining

The heat generated is shared by the chip, cutting tool and the blank. The apportionment of sharing that heat depends upon the configuration, size and thermal conductivity of the tool – work material and the cutting condition. Fig. 3.2 Visualizes that maximum amount of heat is carried away by the flowing chip. From 10 to 20% of the total heat goes into the tool and some heat is absorbed in the blank. With the increase in cutting velocity, the chip shares heat increasingly.

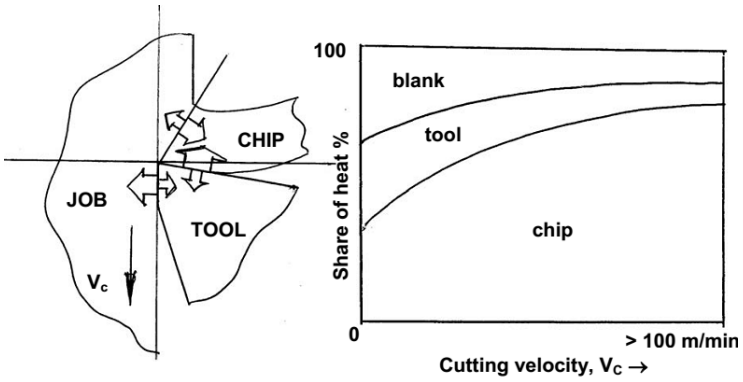

Fig. 3.2 Apportionment of heat amongst chip, tool and blank.

(ii) Effects of the high cutting temperature on tool and job.

The effect of the cutting temperature, particularly when it is high, is mostly detrimental to both the tool and the job. The major portion of the heat is taken away by the chips. But it does not matter because chips are thrown out. So attempts should be made such that the chips take away more and more amount of heat leaving small amount of heat to harm the tool and the job.

The possible detrimental effects of the high cutting temperature on cutting tool (edge) are

- rapid tool wear, which reduces tool life
- plastic deformation of the cutting edges if the tool material is not enough hot-hard and hot-strong
- thermal flaking and fracturing of the cutting edges due to thermal shocks
- built-up-edge formation

The possible detrimental effects of cutting temperature on the machined job are:

- Dimensional inaccuracy of the job due to thermal distortion and expansion-contraction during and after machining.
- Surface damage by oxidation, rapid corrosion, burning etc.
- Induction of tensile residual stresses and micro cracks at the surface / subsurface.

However, often the high cutting temperature helps in reducing the magnitude of the cutting forces and cutting power consumption to some extent by softening or reducing the shear strength, τ_s of the work material ahead the cutting edge. To attain or enhance such benefit the work material ahead the cutting zone is often additionally heated externally. This technique is known as Hot Machining and is beneficially applicable for the work materials which are very hard and hardenable like high manganese steel, Hadfield steel, Nihard, Nimonic etc.

Determination of cutting temperature

The magnitude of the cutting temperature need to be known or evaluated to facilitate

- Assessment of mach inability which is judged mainly by cutting forces and temperature and tool life
- Design and selection of cutting tools
- evaluate the role of variation of the different machining parameters on cutting temperature
- proper selection and application of cutting fluid
- Analysis of temperature distribution in the chip, tool and job.

The temperatures which are of major interests are:

θ_s: Average shear zone temperature

θ_i : Average (and maximum) temperature at the chip-tool interface

θ_f: Temperature at the work-tool interface (tool flanks)

θ_{avg}: Average cutting temperature

Cutting temperature can be determined by two ways:

- Analytically – using mathematical models (equations) if available or can be developed. This method is simple, quick and inexpensive but less accurate and precise.
- Experimentally – this method is more accurate, precise and reliable.

Analytical estimation of cutting temperature, $\boldsymbol{\theta_s}$

Average shear zone temperature, $\boldsymbol{\theta_s}$

Equation(s) have to be developed for the purpose. One simple method is presented here.

The cutting energy per unit time, i.e., $P_z V_c$ gets used to cause primary shear and to overcome friction at the rake face as,

$$P_z.V_c = P_s.V_s + F.V_f \qquad (3.1)$$

Where, V_s = slip velocity along the shear plane

And V_f = average chip – velocity

So, $P_s.V_s = P_z.V_c - F.V_f$

Equating amount of heat received by the chip in one minute from the shear zone and the heat contained by that chip, it appears,

$$\frac{A.q_1(P_z.V_c - F.V_f)}{j} = c_v a_1 b_1 V_c(\theta_s - \theta_a) \quad (3.2)$$

Where, A = fraction (of shear energy that is converted into heat)

q_1= fraction (of heat that goes to the chip from the shear zone)

J = mechanical equivalent of heat of the chip / work material

C_v = volume specific heat of the chip

θ_a= ambient temperature

$a_1.b_1$= cross sectional area of uncut chip

= ts_0

Therefore, $\theta_s = \frac{Aq_1(P_z.V_c - FV_f)}{jtS_0V_c} + \theta_a$ (3.3)

Or, $\theta_s \cong \frac{Aq_{1(P_z - F/\zeta)}}{jtS_0}$ (3.4)

Generally A varies from 0.95 to 1.0 and q from 0.7 to 0.9 in machining like turning.

Average chip – tool interface temperature, $\boldsymbol{\theta_i}$

Using the two dimensionless parameters, θ_1 and θ_2 and their simple relation (Buckingham),

$$\theta_1 = C_1.Q_2^n \quad (3.5)$$

Where, $Q_1 = \left(\frac{C_v\theta_i}{E_c}\right)$ and $Q_2 = \left(\frac{V_c C_v a_1}{\lambda}\right)^{0.5}$

E_C= specific cutting energy

C_v= volume specific heat

λ= thermal conductivity

C_1= a constant

n = an index close to 0.25

Therefore, $\theta_i = C_1 E_C \sqrt{V_c a_1 / \lambda C_v}$ (3.6)

Using equation 3.6 one can estimate the approximate value of average θ_i from the known other machining parameters.

Experimental methods of determination of cutting temperature

Amongθ_s, θ_i, and θ_f, θ_i is obviously the highest one and its value is maximum almost at the middle of the chip – tool contact length. Experimental methods generally provide the average or maximum value of θi. Some techniques also enable get even distribution of temperature in the chip, tool and job at the cutting zone.

The feasible experimental methods are:

- Calorimetric method – quite simple and low cost but inaccurate and gives only grand average value
- Decolorizing agent – some paint or tape, which change in colour with variation of temperature, is pasted on the tool or job near the cutting point; the as such colour of the chip (steels) may also often indicate cutting temperature
- Tool-work thermocouple – simple and inexpensive but gives only average or maximum value
- Moving thermocouple technique
- •Embedded thermocouple technique
- Using compound tool

Indirectly from Hardness and structural transformation

- Photo-cell technique
- Infra ray detection method

The aforesaid methods are all feasible but vary w.r.t. accuracy, preciseness and reliability as well as complexity or difficulties and expensiveness. Some of the methods commonly used are briefly presented here.

Tool work thermocouple technique

Fig. 3.3 shows the principle of this method.

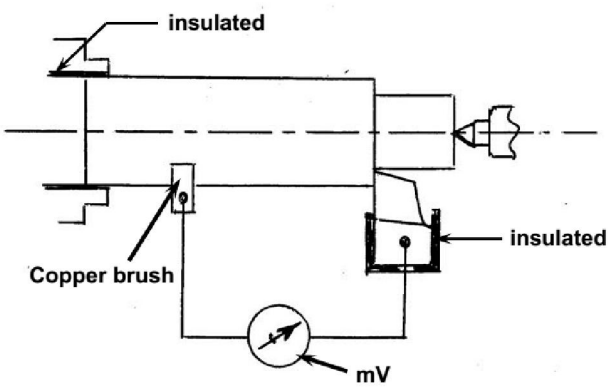

Fig. 3.3 Tool-work thermocouple technique of measuring cutting temperature

In a thermocouple two dissimilar but electrically conductive metals are connected at two junctions. Whenever one of the junctions is heated, the difference in temperature at the hot and cold junctions produce a proportional current which is detected and measured by a milli-voltmeter. In machining like turning, the tool and the job constitute the two dissimilar metals and the cutting zone functions as the hot junction. Then the average cutting temperature is evaluated from the mV after thorough calibration for establishing the exact relation between mV and the cutting temperature.

Fig. 3.4 typically shows a method of calibration for measuring average cutting temperature, θ_{avg} , in turning steel rod by uncoated carbide tool.

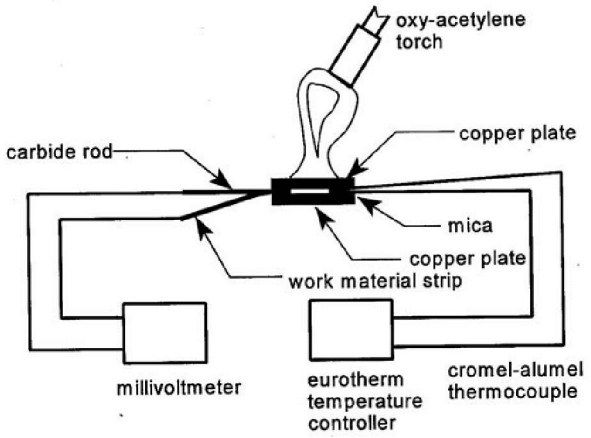

Fig. 3.4 Calibration for tool – work thermocouple.

Moving thermocouple technique

This simple method, schematically shown in Fig. 3.5, enables measure the gradual variation in the temperature of the flowing chip before, during and immediately after its formation. A bead of

standard thermocouple like chromealumel is brazed on the side surface of the layer to be removed from the work surface and the temperature is attained in terms of mV.

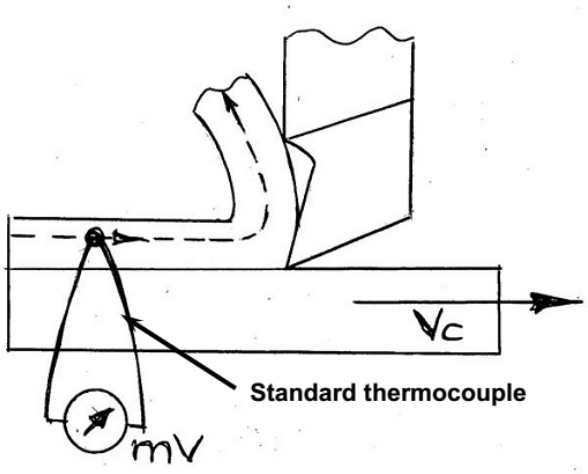

Fig. 3.5 Moving thermocouple technique

Embedded thermocouple technique

In operations like milling, grinding etc. where the previous methods are not applicable, embedded thermocouple can serve the purpose. Fig. 3.6 shows the principle. The standard thermocouple monitors the job temperature at a certain depth, h_i from the cutting zone. The temperature recorded in oscilloscope or strip chart recorder becomes maximum when the thermocouple bead comes nearest (slightly offset) to the grinding zone. With the progress of grinding the depth, h_i gradually decreases after each grinding pass and the value of temperature, θ_m also rises as has been indicated in Fig. 3.6 For getting the temperature exactly at the surface i.e., grinding zone, hi has to be zero, which is not possible. So the θ_m vs h_i curve has to be extrapolated up to h_i= 0 to get the actual grinding zone temperature. Log – log plot helps such extrapolation more easily and accurately.

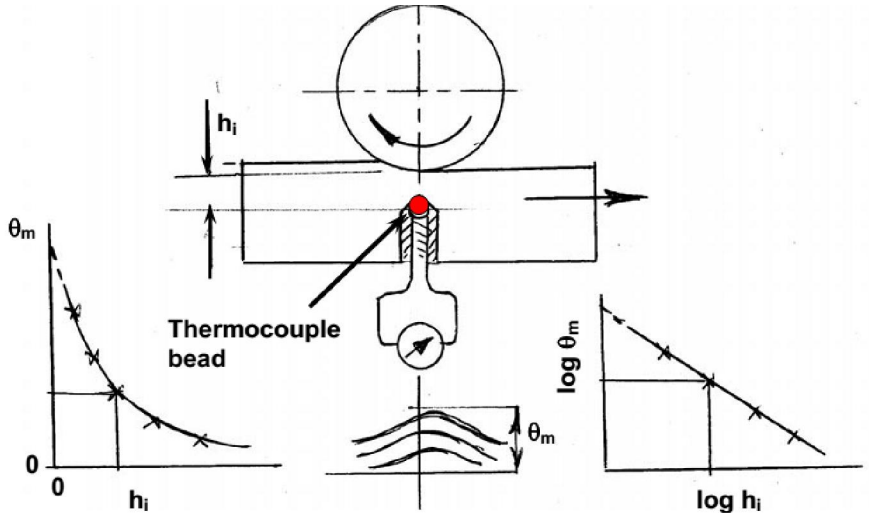

Fig. 3.6 Embedded thermocouple technique

Measurement of chip-tool interface temperature by compound tool

In this method a conducting tool piece (carbide) is embedded in a non conducting tool (ceramic). The conducting piece and the job form the tool work thermocouple as shown in Fig.3.7 which detects temperature θ_i at the location (L_i) of the carbide strip. Thus θican be measured along the entire chip-tool contact length by gradually reducing L_i by grinding the tool flank. Before that calibration has to be done as usual.

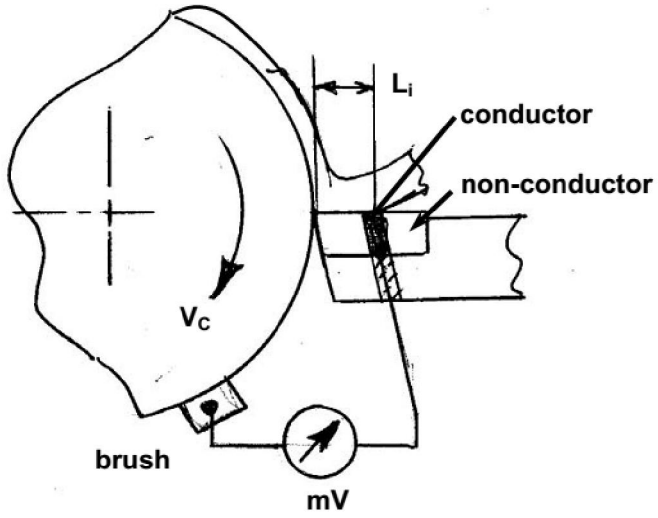

Fig. 3.7 Compound rake used for measuring cutting temperature along rake surface

Photo-cell technique

This unique technique enables accurate measurement of the temperature along the shear zone and tool flank as can be seen in Fig. 3.8. The electrical resistance of the cell, like PbS cell, changes when it is exposed to any heat radiation. The amount of change in the resistance depends upon the temperature of the heat radiating source and is measured in terms of voltage, which is calibrated with the source temperature. It is evident from Fig. 3.8 That the cell starts receiving radiation through the small hole only when it enters the shear zone where the hole at the upper end faces a hot surface. Receiving radiation and measurement of temperature continues until the hole passes through the entire shear zone and then the tool flank.

Infra-red photographic technique

This modern and powerful method is based on taking infra-red photograph of the hot surfaces of the tool, chip, and/or job and get temperature distribution at those surfaces. Proper calibration is to be done before that. The fringe pattern readily changes with the change in any machining parameter which affect cutting temperature.

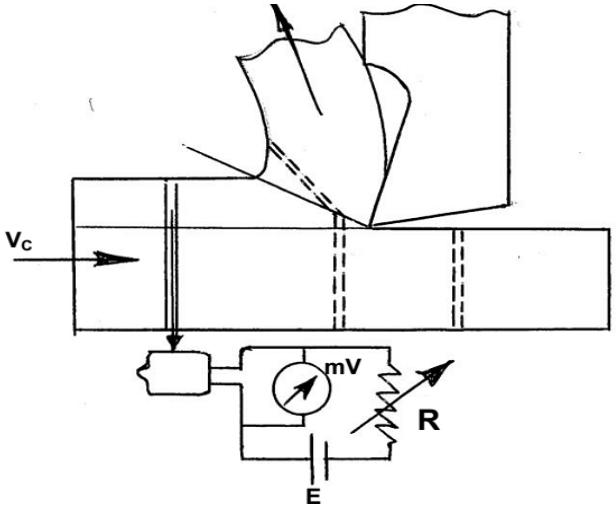

Fig. 3.8 measuring temperature at shear plane and tool flank by photocell technique

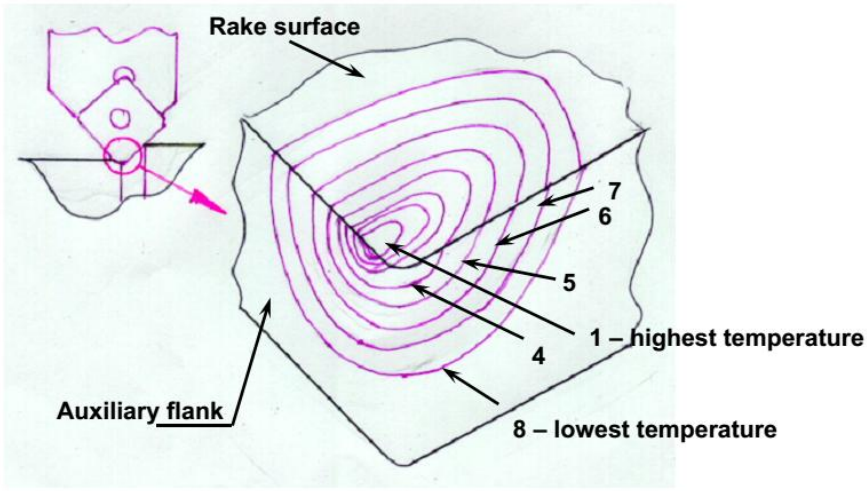

Fig. 3.9 Temperature distribution at the tool tip detected by Infra ray technique

Role of variation of the various machining parameters on cutting temperature

The magnitude of cutting temperature is more or less governed or influenced by all the machining parameters like:

- Work material: - specific energy requirement
  - Ductility
  - Thermal properties (λ, C_v)
- Process parameters: - cutting velocity (V_C)
  - feed (S_0)
  - Depth of cut (t)
- cutting tool material: - thermal properties
  - wear resistance
  - Chemical stability
- Tool geometry: - rake angle (γ)
  - Cutting edge angle (φ)
  - Clearance angle (α)
  - nose radius (r)
- cutting fluid : - thermal and lubricating properties

- Method of application

Many researchers studied, mainly experimentally, on the effects of the various parameters on cutting temperature. A well established overall empirical equation is,

$$\theta_i = \frac{C_\theta (V_c)^{0.4} (S_0 \sin\theta)^{0.24} (t)^{0.105}}{\left(\frac{t}{S_0}\right)^{0.086} (r)^{0.11} (tS_0)^{0.054}} \quad (3.7)$$

Where, C_θ = a constant depending mainly on the work-tool materials Equation 3.7 clearly indicates that among the process parameters V_C affects θ_i most significantly and the role of t is almost insignificant. Cutting temperature depends also upon the tool geometry. Equation 3.7 depicts that θ_i can be reduced by lowering the principal cutting edge angle, φ and increasing nose radius, r. Besides that the tool rake angle, γ and hence inclination angle, λ also have significant influence on the cutting temperature.

Increase in rake angle will reduce temperature by reducing the cutting forces but too much increase in rake will raise the temperature again due to reduction in the wedge angle of the cutting edge.

Proper selection and application of cutting fluid help reduce cutting temperature substantially through cooling as well as lubrication.

Control of cutting temperature

It is already seen that high cutting temperature is mostly detrimental in several respects. Therefore, it is necessary to control or reduce the cutting temperature as far as possible.

Cutting temperature can be controlled in varying extent by the following general methods:

- proper selection of material and geometry of the cutting tool(s)
- optimum selection of $V_C - S_0$ combination without sacrificing MRR
- proper selection and application of cutting fluid
- Application of special technique, if required and feasible.

Basic methods of controlling cutting temperature

It is already realized that the cutting temperature, particularly when it is quite high, is very detrimental for both cutting tools and the machined jobs and hence need to be controlled, i.e., reduced as far as possible without sacrificing productivity and product quality.

The methods generally employed for controlling machining temperature and its detrimental effects are :

- Proper selection of cutting tools; material and geometry
- Proper selection of cutting velocity and feed
- Proper selection and application of cutting fluid

Selection of material and geometry of cutting tool for reducing cutting temperature and its effects

Cutting tool material may play significant role on reduction of cutting temperature depending upon the work material.

As for example,

- PVD or CVD coating of HSS and carbide tools enables reduce cutting temperature by reducing friction at the chip-tool and work-tool interfaces.
- In high speed machining of steels lesser heat and cutting temperature develop if machined by CBN tools which produce lesser cutting forces by retaining its sharp geometry for its extreme hardness and high chemical stability.
- The cutting tool temperature of ceramic tools decrease further if the thermal conductivity of such tools is enhanced (by adding thermally conductive materials like metals, carbides, etc in Al2O3or Si3N4)
- Cutting temperature can be sizeably controlled also by proper selection of the tool geometry in the following ways;
- large positive tool–rake helps in reducing heat and temperature generation by reducing the cutting forces, but too much increase in rake mechanically and thermally weakens the cutting edges
- compound rake, preferably with chip–breaker, also enables reduce heat and temperature through reduction in cutting forces and friction
- even for same amount of heat generation, the cutting temperature decreases with the decrease in the principal cutting edge angle, φ as
- $\theta_C \; \alpha \; [V_C^{0.5}(S_0 \sin\theta)^{0.25}]$ (3.8)
- Nose radius of single point tools not only improves surface finish but also helps in reducing cutting temperature to some extent.

Selection of cutting velocity and feed

Cutting temperature can also be controlled to some extent, even without sacrificing MRR, by proper or optimum selection of the cutting velocity and feed within their feasible ranges. The rate of heat generation and hence cutting temperature are governed by the amount of cutting power consumption, P_C where;

$$P_C = P_Z.V_C = tS_0\tau_S f V_C \quad (3.9)$$

So apparently, increase in both so and V_C raise heat generation proportionately. But increase inV_C, though further enhances heat generation by faster rubbing action, substantially reduces cutting forces, hence heat generation by reducing τ_S and also the form factor f. The overall relative effects of variation of V_C and S_0 on cutting temperature will depend upon other machining conditions. Hence, depending upon the situation, the cutting temperature can be controlled significantly by optimum combination of V_C and S_0 for a given MRR.

Control of cutting temperature by application of cutting fluid

Cutting fluid, if employed, reduces cutting temperature directly by taking away the heat from the cutting zone and also indirectly by reducing generation of heat by reducing cutting forces.

Purposes of application of cutting fluid in machining and grinding.

The basic purposes of cutting fluid application are :

- Cooling of the job and the tool to reduce the detrimental effects of cutting temperature on the job and the tool
- Lubrication at the chip–tool interface and the tool flanks to reduce cutting forces and friction and thus the amount of heat generation.
- Cleaning the machining zone by washing away the chip – particles and debris which, if present, spoils the finished surface and accelerates damage of the cutting edges
- Protection of the nascent finished surface – a thin layer of the cutting fluid sticks to the machined surface and thus prevents its harmful contamination by the gases like SO2, O2, H_2S, N_XO_Y present in the atmosphere.

However, the main aim of application of cutting fluid is to improve machinability through reduction of cutting forces and temperature, improvement by surface integrity and enhancement of tool life.

Essential properties of cutting fluids

To enable the cutting fluid fulfill its functional requirements without harming the Machine – Fixture – Tool – Work (M-F-T-W) system and the operators, the cutting fluid should possess the following properties:

- For cooling :
    - high specific heat, thermal conductivity and film coefficient for heat transfer
    - spreading and wetting ability

- For lubrication :
    - high lubricity without gumming and foaming
    - wetting and spreading
    - high film boiling point
    - friction reduction at extreme pressure (EP) and temperature
- Chemical stability, non-corrosive to the materials of the M-F-T-W system
- less volatile and high flash point
- high resistance to bacterial growth
- odorless and also preferably colorless
- non toxic in both liquid and gaseous stage
- easily available and low cost.

Principles of cutting fluid action

The chip-tool contact zone is usually comprised of two parts; plastic or bulk contact zone and elastic contact zone as indicated in Fig. 3.10

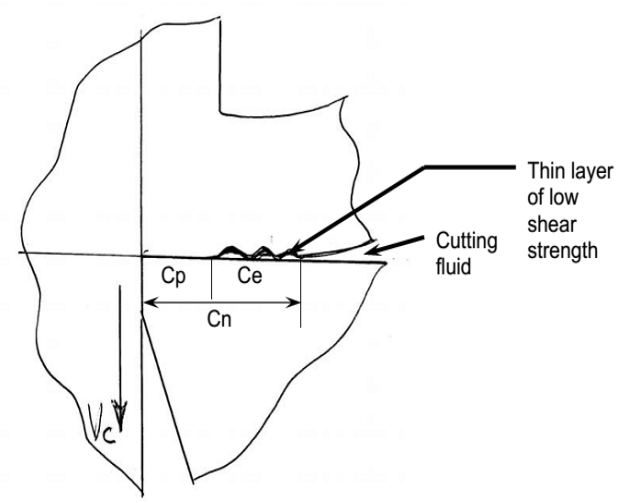

Fig. 3.10 Cutting fluid action in machining.

The cutting fluid cannot penetrate or reach the plastic contact zone but enters in the elastic contact zone by capillary effect. With the increase in cutting velocity, the fraction of plastic contact zone gradually increases and covers almost the entire chip-tool contact zone as indicated in Fig. 3.12. Therefore, at high speed machining, the cutting fluid becomes unable to lubricate and cools the tool and the job only by bulk external cooling.

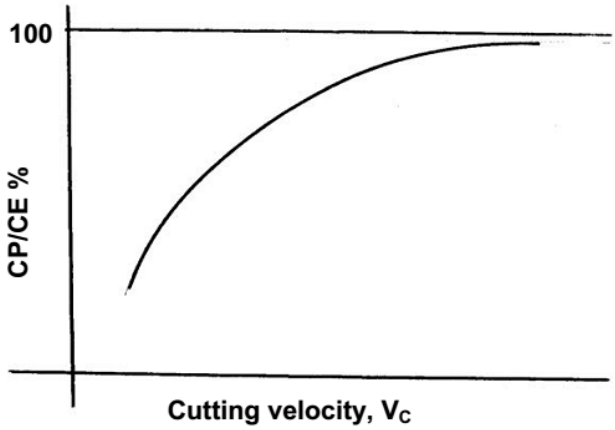

Fig. 3.12 Apportionment of plastic and elastic contact zone with increase in cutting velocity.

The chemicals like chloride, phosphate or sulphide present in the cutting fluid chemically reacts with the work material at the chip undersurface under high pressure and temperature and forms a thin layer of the reaction product. The low shear strength of that reaction layer helps in reducing friction.

To form such solid lubricating layer under high pressure and temperature some extreme pressure additive (EPA) is deliberately added in reasonable amount in the mineral oil or soluble oil.

For extreme pressure, chloride, phosphate or sulphide type EPA is used depending upon the working temperature, i.e. moderate (200^0C ~350^0C), high (350^0C ~500^0C) and very high (500^0C ~800^0C) respectively.

Types of cutting fluids and their application

Generally, cutting fluids are employed in liquid form but occasionally also employed in gaseous form. Only for lubricating purpose, often solid lubricants are also employed in machining and grinding.

The cutting fluids, which are commonly used, are:

• Air blast or compressed air only.

Machining of some materials like grey cast iron become inconvenient or difficult if any cutting fluid is employed in liquid form. In such case only air blast is recommended for cooling and cleaning

• Water

For its good wetting and spreading properties and very high specific heat, water is considered as the best coolant and hence employed where cooling is most urgent.

• Soluble oil

Water acts as the best coolant but does not lubricate. Besides, use of only water may impair the machine-fixture-tool-work system by rusting So oil containing some emulsifying agent and additive like EPA, together called cutting compound, is mixed with water in a suitable ratio (1 ~ 2 in 20 ~ 50). This milk like white emulsion, called soluble oil, is very common and widely used in machining and grinding.

• Cutting oils

Cutting oils are generally compounds of mineral oil to which are added desired type and amount of vegetable, animal or marine oils for improving spreading, wetting and lubricating properties. As and when required some EP additive is also mixed to reduce friction, adhesion and BUE formation in heavy cuts.

• Chemical fluids

These are occasionally used fluids which are water based where some organic and or inorganic materials are dissolved in water to enable desired cutting fluid action.

There are two types of such cutting fluid;

– Chemically inactive type – high cooling, anti-rusting and wetting but less lubricating

– Active (surface) type – moderate cooling and lubricating.

• Solid or semi-solid lubricant

Paste, waxes, soaps, graphite, Moly-disulphide (MoS_2) may also often be used, either applied directly to the work piece or as an impregnant in the tool to reduce friction and thus cutting forces, temperature and tool wear.

• Cryogenic cutting fluid

Extremely cold (cryogenic) fluids (often in the form of gases) like liquid CO_2or $N_2$are used in some special cases for effective cooling without creating much environmental pollution and health hazards.

Selection of Cutting Fluid

The benefit of application of cutting fluid largely depends upon proper selection of the type of the cutting fluid depending upon the work material, tool material and the machining condition. As for example, for high speed machining of not-difficult-to-machine materials greater cooling type fluids are preferred and for low speed machining of both conventional and difficult-to machine materials greater lubricating type fluid is preferred. Selection of cutting fluids for machining some common engineering materials and operations are presented as follows :

• **Grey cast iron**: Generally dry for its self lubricating propertyAir blast for cooling and flushing chips.Soluble oil for cooling and flushing chips in high speed machining and grinding

• **Steels :** if machined by HSS tools, sol. Oil (1: 20 ~30) for low carbon and alloy steels and neat oil with EPA for heavy cuts .If machined by carbide tools thinner sol. Oil for low strength steel, thicker sol.Oil (1:10 ~ 20) for stronger steels and staright sulphurised oil for heavy and low speed cuts and EP cutting oil for high alloy steel. Often steels are machined dry by carbide tools for preventing thermal shocks.

•**Aluminium and its alloys:** Preferably machined dry Light but oily soluble oil Straight neat oil or kerosene oil for stringent cuts.

• **Copper and its alloys:** Water based fluids are generally used Oil with or without inactive EPA for tougher grades of Cu-alloy.

• **Stainless steels and**

Heat resistant alloys: High performance soluble oil or neat oil with high concentration with chlorinated EP additive.

The brittle ceramics and cermets should be used either under dry condition or light neat oil in case of fine finishing.

Grinding at high speed needs cooling (1:50 ~ 100) soluble oil. For finish grinding of metals and alloys low viscosity neat oil is also used.

MODULE-4

Concept, definition and criteria of judgment of machinability

It is already known that preformed components are essentially machined to impart dimensional accuracy and surface finish for desired performance and longer service life of the product. It is obviously attempted to accomplish machining effectively, efficiently and economically as far as possible by removing the excess material smoothly and speedily with lower power consumption, tool wear and surface deterioration. But this may not be always and equally possible for all the work materials and under all the conditions. The machining characteristics of the work materials widely vary and also largely depend on the conditions of machining. A term; 'Machinability' has been introduced for gradation of work materials w.r.t. machining characteristics.

But truly speaking, there is no unique or clear meaning of the term machinability. People tried to describe "Machinability" in several ways such as:

- It is generally applied to the machining properties of work material
- It refers to material (work) response to machining
- It is the ability of the work material to be machined
- It indicates how easily and fast a material can be machined.

But it has been agreed, in general, that it is difficult to clearly define and quantify Machinability. For instance, saying 'material A is more machinable than material B' may mean that compared to 'B',

- 'A' causes lesser tool wear or longer tool life
- 'A' requires lesser cutting forces and power
- 'A' provides better surface finish

Where, surface finish and tool life are generally considered more important in finish machining and cutting forces or power in bulk machining. Machining is so complex and dependant on so many factors that the order of placing the work material in a group, w.r.t. favourable behaviour in machining, will change if the consideration is changed from tool life to cutting power or surface quality of the product and vice versa. For instance, the machining behaviour of work materials are so affected by the cutting tool; both material and geometry, that often machinability is expressed as "operational characteristics of the work-tool combination". Attempts were made to measure or quantify machinability and it was done mostly in terms of:

- Tool life which substantially influences productivity and economy in machining
- Magnitude of cutting forces which affects power consumption and dimensional accuracy
- Surface finish which plays role on performance and service life of the product.

Often cutting temperature and chip form are also considered for assessing machinability.

But practically it is not possible to use all those criteria together for expressing machinability quantitatively. In a group of work materials a particular one may appear best in respect of, say, tool life but may be much poor in respect of cutting forces and surface finish and so on. Besides that, the machining responses of any work material in terms of tool life, cutting forces, surface finish etc. are more or less significantly affected by the variation; known or unknown, of almost all the parameters or factors associated with machining process. Machining response of a material may also change with the processes, i.e. turning, drilling, milling etc. therefore, there cannot be as such any unique value to express machinability of any material, and machinability, if to be used at all, has to be done for qualitative assessment.

However, earlier, the relative machining response of the work materials compared to that of a standard metal was tried to be evaluated quantitatively only based on tool life (VB* = 0.33 mm) by an index, Machinability rating (MR)

$$= \frac{speed\ (f_{pm}) of\ machining\ the\ work\ giving\ 60\ \text{min}\ tool\ life}{speed\ (f_{pm})\ of\ machining\ the\ standard\ metal\ giving\ 60\ \text{min}\ tool\ life} \times 100$$

Fig. 4.1 shows such scheme of evaluating Machinability rating (MR) of any work material. The free cutting steel, AISI – 1112, when machined (turned) at 100 fpm, provided 60 min of tool life. If the work material to be tested provides 60 min of tool life at cutting velocity of 60 fpm (say), as indicated in Fig. 4.1, under the same set of machining condition, then machinability (rating) of that material would be,

$MR = \frac{60}{100} \times 100 = 60\%$ or simply 60 (based on 100% for the standard material)

or, simply the value of the cutting velocity expressed in fpm at which a work material provides 60 min tool life was directly considered as the MR of that work material. In this way the MR of some materials, for instance, were evaluated as,

Metal	MR
Ni	200
Br	300
Al	200
Cl	70
Inconel	30

But usefulness and reliability of such practice faced several genuine doubts and questions:

- Tool life cannot or should not be considered as the only criteria for judging machinability.
- under a given condition a material can yield different tool life even at a fixed speed (cutting velocity); exact composition, microstructure, treatments etc. of that material may cause significant difference in tool life
- The tool life - speed relationship of any material may substantially change with the variation in
    - material and geometry of the cutting tool
    - level of process parameters (V_c, s_o, t)
    - machining environment (cutting fluid application)
    - machine tool condition

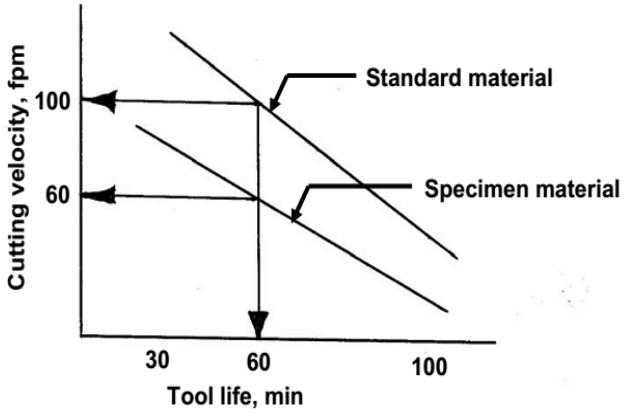

Fig. 4.1 Machinability rating in terms of cutting velocity giving 60 min tool life.

Keeping all such factors and limitations in view, Machinability can be tentatively defined as "ability of being machined" and more reasonably as "ease of machining".

Such ease of machining or machinability characteristics of any tool-work pair is to be judged by:

- magnitude of the cutting forces
- tool wear or tool life
- surface finish
- magnitude of cutting temperature
- chip forms

Machinability will be considered desirably high when cutting forces, temperature, surface roughness and tool wear are less, tool life is long and chips are ideally uniform and short enabling short chip-tool contact length and less friction.

Role of Variation of the Different Machining Parameters or Factors on Machinability of Work Materials.

The machinability characteristics and their criteria, i.e., the magnitude of cutting forces and temperature, tool life and surface finish are governed or influenced more or less by all the variables and factors involved in machining such as,

(a) Properties of the work material

(b) Cutting tool; material and geometry

(c) Levels of the process parameters

(d) Machining environments (cutting fluid application etc)

Machinability characteristics of any work – tool pair may also be further affected by,

- strength, rigidity and stability of the machine
- kind of machining operations done in a given machine tool
- Functional aspects of the special techniques, if employed.

(a) Role of the properties of the work material on machinability.

The work material properties that generally govern machinability in varying extent are:

- The basic nature – brittleness or ductility etc.
- microstructure
- mechanical strength – fracture or yield
- hardness
- hot strength and hot hardness
- work hardenability
- thermal conductivity
- chemical reactivity
- stickiness / self lubricit

Machining of brittle and ductile materials

In general, brittle materials are relatively more easily machinable for:

- the chip separation is effected by brittle fracture requiring lesser energy of chip formation

- ❖ shorter chips causing lesser frictional force and heating at the rake surface

For instance, compared to even mild steel, grey cast iron jobs produce much lesser cutting forces and temperature .Smooth and continuous chip formation is likely to enable mild steel produce better surface finish but BUE, if formed, may worsen the surface finish.For machining, like turning of ductile metals, the expression

$$P_Z = tS_0\tau_S f \quad (4.1)$$

Indicates that cutting forces increase with the increase in yield shear strength, τ_S of the work material. The actual value of τ_S of any material, again, changes with the condition of machining and also on the ductility of the work material as,

$$\tau_S = 0.74\sigma_U \varepsilon^{0.6\Delta} \quad (4.2)$$

where,

σ_U = ultimate tensile strength which is a classical property of the material

Δ= percentage elongation indicating ductility of the work material

ε = cutting strain

Role of cutting tool material and geometry on machinability of any work material.

Role of tool materials

In machining a given material, the tool life is governed mainly by the tool material which also influences cutting forces and temperature as well as accuracy and finish of the machined surface. The composition, microstructure, strength, hardness, toughness, wear resistance, chemical stability and thermal conductivity of the tool material play significant roles on the

machinability characteristics though in different degree depending upon the properties of the work material.

Fig. 4.2 schematically shows how in turning materials like steels, the tool materials affect tool life at varying cutting velocity. High wear resistance and chemical stability of the cutting tools like coated carbides, ceramics, cubic Boron nitride (CBN) etc also help in providing better surface integrity of the product by reducing friction, cutting temperature and BUE formation in high speed machining of steels. Very soft, sticky and chemically reactive material like pure aluminium attains highest machinability when machined by diamond tools.

Role of the geometry of cutting tools on machinability.

The geometrical parameters of cutting tools (say turning tool) that significantly affect the machinability of a given work material (say mild steel) under given machining conditions in terms of specific energy requirement, tool life, surface finish etc. are:

- Tool rake angles (γ)
- Clearance angle (α)
- cutting angles (φ and φ_1)
- Nose radius (r)

The other geometrical (tool) parameters that also influence machinability to some extent directly and indirectly are:

–inclination angle (λ)

– edge beveling or rounding (r′)

– Depth, width and form of integrated chip breaker

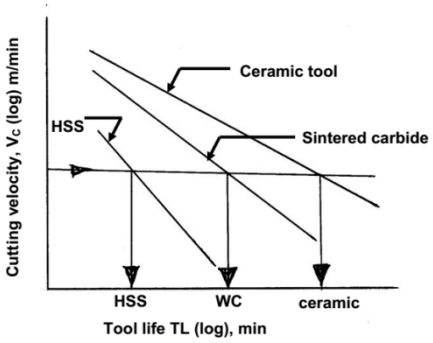

Fig. 4.2Role of cutting tool material on machinability (tool life)

Effects of tool rake angle(s) on machinability

In machining like turning ductile material, the main cutting force, P_Z decreases as typically shown in Fig. 4.3 mainly due to,

$$P_Z = tS_0\tau_S f \tag{4.3}$$

Where, $f = \zeta - \tan\gamma + 1$

$\zeta = e^{\mu(\pi/2-\gamma)}$

$\tau_S = 0.74\sigma_U \varepsilon^{0.6\Delta}$

$$\varepsilon = \zeta - \tan\gamma$$

The expressions clearly show that increase in γ reduces P_Z through reduction in cutting strain (ε), chip reduction coefficient (ζ) and hence τ_S and the form factor, f. With P_Z , P_{XY} also decreases proportionally. But too much increase in rake weakens the cutting edge both mechanically and thermally and may cause premature failure of the tool. Presence of inclination angle, λ enhances effective rake angle and thus helps in further reduction of the cutting forces. However, the tool rake angle does not affect surface finish that significantly.

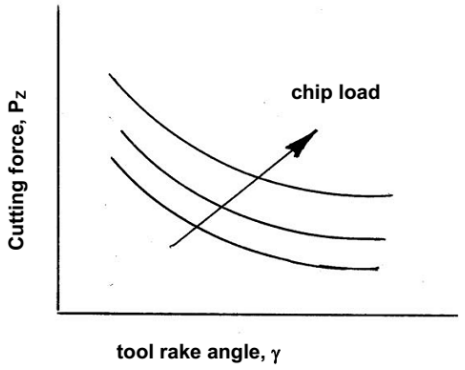

Fig. 4.3Effect of tool rake angle on machinability (cutting force, P_Z)

Role of cutting angles (φ andφ_1) on machinability

The variation in the principal cutting edge angle, φ does not affect P_Z or specific energy requirement but influences P_Y and the cutting temperature (θ_C) quite significantly as indicated in Fig. 4.4 mainly for,

$$P_Y = P_{XY}\cos\varphi \text{ i.e., } \alpha P_Z \cos\varphi \qquad (4.4)$$

$$\text{And } \theta_C\ \alpha\ \sqrt{V_C\, S_0 \sin\varphi} \qquad (4.5)$$

The force, P_Y , if large, may impair the product quality by dimensional deviation and roughening the surface due to vibration.

Reduction in both φ and φ_1 improves surface finish sizeably in continuous chip formation, as

$$h_{max} = \frac{S_0}{\cot\varphi + \cot\varphi_1} \qquad (4.6)$$

where h_{max} is the maximum surface roughness due to feed marks alone.

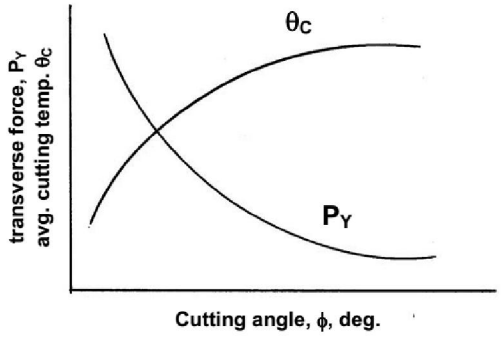

Fig. 4.4 Effects of variation in cutting angle on machinability (θ_C and P_Y)

Effects of clearance angle (α)

Fig. 4.5 schematically shows how clearance angle, α affects tool life.

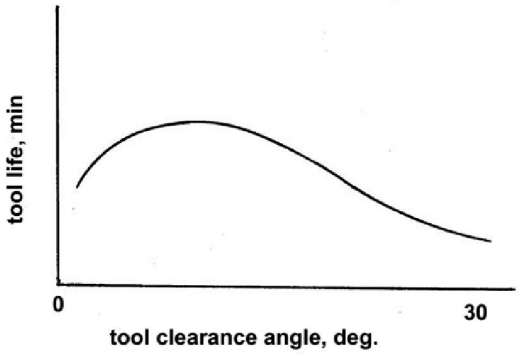

Fig. 4.5Influence of tool clearance angle on tool life.

Inadequate clearance angle reduces tool life and surface finish by tool - work rubbing, and again too large clearance reduces the tool strength and hence tool life.

Role of tool nose radius (r) on machinability

Proper tool nose radiusing improves machinability to some extent through

- Increase in tool life by increasing mechanical strength and reducing temperature at the tool tip
- Reduction of surface roughness, h_{max}
- As $h_{max} = \frac{(S_0)^2}{8r}$ (4.7)

Proper edge radiusing (r′) also often enhances strength and life of the cutting edge without much increase in cutting forces.

(c) Role of the process parameters on machinability

Proper selection of the levels of the process parameters (V_C, S_0 and t) can provide better machinability characteristics of a given work – tool pair even without sacrificing productivity or MRR.

Amongst the process parameters, depth of cut, t plays least significant role and is almost invariable. Compared to feed (S_0) variation of cutting velocity (V_C) governs machinability more predominantly. Increase in V_C , in general, reduces tool life but it also reduces cutting forces or specific energy requirement and improves surface finish through favourable chip-tool interaction. Some cutting tools, especially ceramic tools perform better and last longer at higher V_C within limits. Increase in feed raises cutting forces proportionally but reduces specific energy requirement to some extent. Cutting temperature is also lesser susceptible to increase in S_0 than V_C . But increase in S_0 , unlike V_C raises surface roughness. Therefore, proper increase in V_C , even at the expense of S_0 often can improve machinability quite significantly.

(d) Effects of machining environment (cutting fluids) on machinability

The basic purpose of employing cutting fluid is to improve machinability characteristics of any work – tool pair through:

- improving tool life by cooling and lubrication
- reducing cutting forces and specific energy consumption
- improving surface integrity by cooling, lubricating and cleaning at the cutting zone

The favourable roles of cutting fluid application depend not only on its proper selection based on the work and tool materials and the type of the machining process but also on its rate of flow, direction and location of application.

Possible Ways of Improving Machinability Of Work Materials

- The machinability of the work materials can be more or less improved, without sacrificing productivity, by the following ways:
- Favorable change in composition, microstructure and mechanical properties by mixing suitable type and amount of additive(s) in the work material and appropriate heat treatment
- Proper selection and use of cutting tool material and geometry depending upon the work material and the significant machinability criteria under consideration
- Optimum selection of V_C and S_0 based on the tool – work materials and the primary objectives.

- ❖ Proper selection and appropriate method of application of cutting fluid depending upon the tool – work materials, desired levels of productivity i.e., V_C and S_0 and also on the primary objectives of the machining work undertaken
- ❖ Proper selection and application of special techniques like dynamic machining, hot machining, cryogenic machining etc, if feasible, economically viable and eco-friendly

Failure of cutting tools

Smooth, safe and economic machining necessitate

- ❖ Prevention of premature and catastrophic failure of the cutting tools
- ❖ Reduction of rate of wear of tool to prolong its life

To accomplish the aforesaid objectives one should first know why and how the cutting tools fail.

Cutting tools generally fail by:

1. Mechanical breakage due to excessive forces and shocks. Such kinds of tool failure are random and catastrophic in nature and hence are extremely detrimental.
2. Quick dulling by plastic deformation due to intensive stresses and temperature. This type of failure also occurs rapidly and is quite detrimental and unwanted.
3. Gradual wear of the cutting tool at its flanks and rake surface.

The first two modes of tool failure are very harmful not only for the tool but also for the job and the machine tool. Hence these kinds of tool failure need to be prevented by using suitable tool materials and geometry depending upon the work material and cutting condition. But failure by gradual wear, which is inevitable, cannot be prevented but can be slowed down only to enhance the service life of the tool. The cutting tool is withdrawn immediately after it fails or, if possible, just before it totally fails. For that one must understand that the tool has failed or is going to fail shortly.

Mechanisms and pattern (geometry) of cutting tool wear

For the purpose of controlling tool wear one must understand the various mechanisms of wear that the cutting tool undergoes under different conditions. The common mechanisms of cutting tool wear are:

1. Mechanical wear
    a. thermally insensitive type; like abrasion, chipping and de-lamination
    b. Thermally sensitive type; like adhesion, fracturing, flaking etc.
2. Thermo chemical wear
    a. macro-diffusion by mass dissolution
    b. micro-diffusion by atomic migration

3. Chemical wear
4. Galvanic wear

In diffusion wear the material from the tool at its rubbing surfaces, particularly at the rake surface gradually diffuses into the flowing chips either in bulk or atom by atom when the tool material has chemical affinity or solid solubility towards the work material. The rates of such tool wear increases with the increase in temperature at the cutting zone.

Diffusion wear becomes predominant when the cutting temperature becomes very high due to high cutting velocity and high strength of the work material. Chemical wear, leading to damages like grooving wear may occur if the tool material is not enough chemically stable against the work material and/or the atmospheric gases.

Galvanic wear, based on electrochemical dissolution, seldom occurs when both the work tool materials are electrically conductive, cutting zone temperature is high and the cutting fluid acts as an electrolyte.

The usual pattern or geometry of wear of turning and face milling inserts are typically shown in Fig. 4.6 (a and b) and Fig. 4.7 respectively.

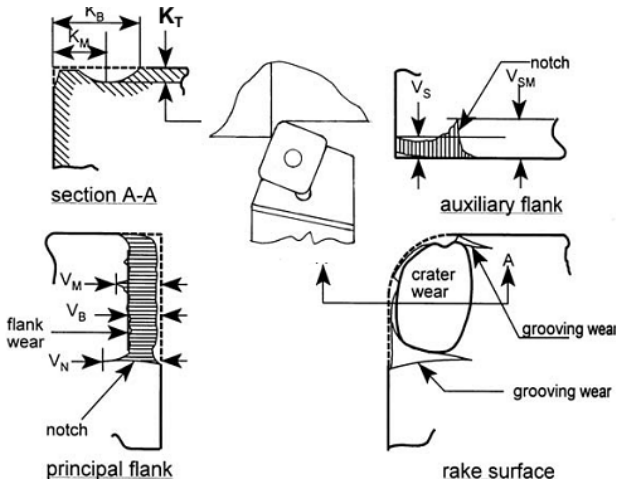

Fig. 4.6 (a) Geometry and major features of wear of turning tools

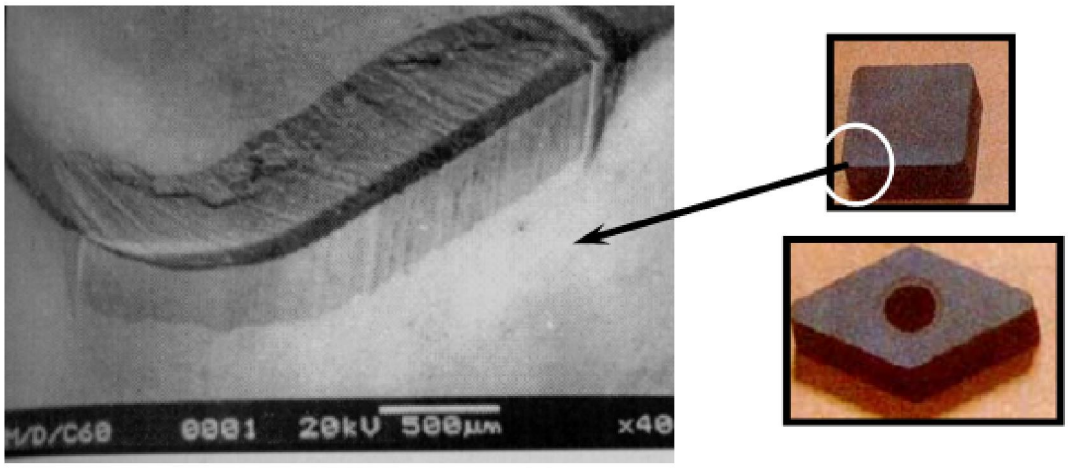

Fig. 4.6 (b) Photographic view of the wear pattern of a turning tool insert

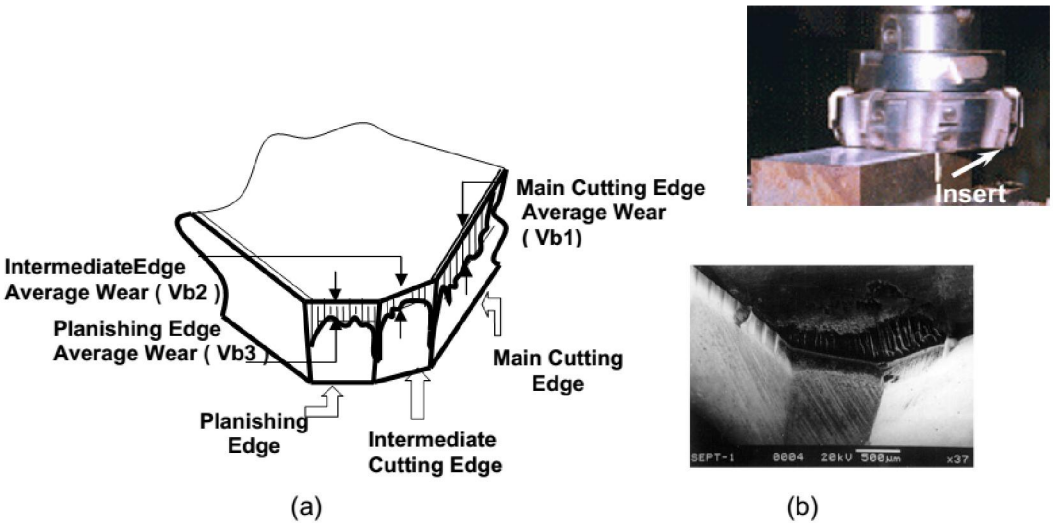

Fig. 4.7 Schematic (a) and actual view (b) of wear pattern of face milling insert

In addition to ultimate failure of the tool, the following effects are also caused by the growing tool-wear:

- increase in cutting forces and power consumption mainly due to the principal flank wear
- increase in dimensional deviation and surface roughness mainly due to wear of the tool-tips and auxiliary flank wear (Vs)
- odd sound and vibration
- worsening surface integrity
- Mechanically weakening of the tool tip.

(iii) Essential properties for cutting tool materials

The cutting tools need to be capable to meet the growing demands for higher productivity and economy as well as to machine the exotic materials which are coming up with the rapid progress in science and technology. The cutting tool material of the day and future essentially require the following properties to resist or retard the phenomena leading to random or early tool failure:

i. high mechanical strength; compressive, tensile, and TRA
ii. fracture toughness – high or at least adequate
iii. high hardness for abrasion resistance
iv. high hot hardness to resist plastic deformation and reduce wear rate at elevated temperature
v. chemical stability or inertness against work material, atmospheric gases and cutting fluids
vi. resistance to adhesion and diffusion
vii. thermal conductivity – low at the surface to resist incoming of heat and high at the core to quickly dissipate the heat entered
viii. high heat resistance and stiffness
ix. Manufacturability, availability and low cost.

Tool Life

Definition –

Tool life generally indicates the amount of satisfactory performance or service rendered by a fresh tool or a cutting point till it is declared failed.

Tool life is defined in two ways:

a) Actual machining time (period) by which a fresh cutting tool (or point) satisfactorily works after which it needs replacement or reconditioning. The modern tools hardly fail prematurely or abruptly by mechanical breakage or rapid plastic deformation. Those fail mostly by wearing process which systematically grows slowly with machining time. In that case, tool life means the span of actual machining time by which a fresh tool can work before attaining the specified limit of tool wear. Mostly tool life is decided by the machining time till flank wear, VB reaches 0.3 mm or crater wear, KT reaches 0.15 mm.
b) The length of time of satisfactory service or amount of acceptable output provided by a fresh tool prior to it is required to replace or recondition.

Assessment of tool life Tool life is always assessed or expressed by span of machining time in minutes, whereas, in industries besides machining time in minutes some other means are also used to assess tool life, depending upon the situation, such as

- ❖ no. of pieces of work machined
- ❖ total volume of material removed
- ❖ Total length of cut.

Measurement of tool wear

The various methods are:

i. By loss of tool material in volume or weight, in one life time – this method is crude and is generally applicable for critical tools like grinding wheels.
ii. by grooving and indentation method – in this approximate method wear depth is measured indirectly by the difference in length of the groove or the indentation outside and inside the worn area
iii. using optical microscope fitted with micrometer – very common and effective method
iv. using scanning electron microscope (SEM) – used generally, for detailed study; both qualitative and quantitative
v. Talysurf, especially for shallow crater wear.

Taylor's tool life equation.

Wear and hence tool life of any tool for any work material is governed mainly by the level of the machining parameters i.e., cutting velocity, (V_C), feed, (S_0) and depth of cut (t). Cutting velocity affects maximum and depth of cut minimum.

The usual pattern of growth of cutting tool wear (mainly VB), principle of assessing tool life and its dependence on cutting velocity are schematically shown in Fig.4.8.

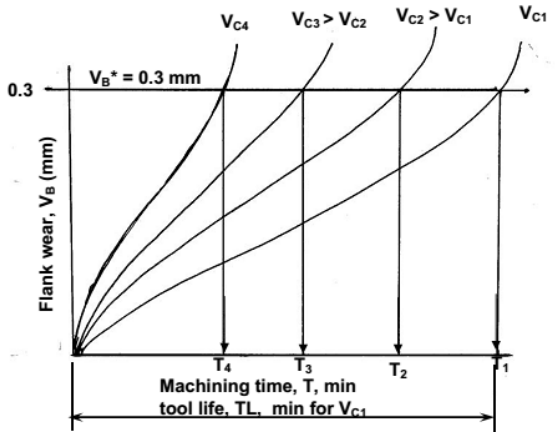

Fig. 4.8 Growth of flank wear and assessment of tool life

The tool life obviously decreases with the increase in cutting velocity keeping other conditions unaltered as indicated in Fig. 4.8.

If the tool lives, T_1, T_2, T_3, T_4 etc are plotted against the corresponding cutting velocities, V_1, V_2, V_3, V_4 etc as shown in Fig. 4.9, a smooth curve like a rectangular hyperbola is found to appear. When F. W. Taylor plotted the same figure taking both V and T in log-scale, a more distinct linear relationship appeared as schematically shown in Fig. 4.10.

With the slope, n and intercept, c, Taylor derived the simple equation as

$$VT^n = C$$

Where, n is called, Taylor's tool life exponent. The values of both 'n' and 'c' depend mainly upon the tool-work materials and the cutting environment (cutting fluid application). The value of C depends also on the limiting value of V_B undertaken (i.e., 0.3 mm, 0.4 mm, 0.6 mm etc.).

Modified Taylor's Tool Life equation

In Taylor's tool life equation, only the effect of variation of cutting velocity, V_C on tool life has been considered. But practically, the variation in feed (so) and depth of cut (t) also play role on tool life to some extent.

Taking into account the effects of all those parameters, the Taylor's tool life equation has been modified as,

$$TL = \frac{C_T}{{V_C}^X {S_0}^Y t^Z}$$

where, TL = tool life in min

C_T –a constant depending mainly upon the tool – work materials and the limiting value of V_B undertaken.

x, y and z –exponents so called tool life exponents depending upon the tool – work materials and the machining environment.

Generally, x > y > z as V_C affects tool life maximum and t minimum.

The values of the constants, CT, x, y and z are available in Machining Data Handbooks or can be evaluated by machining tests.

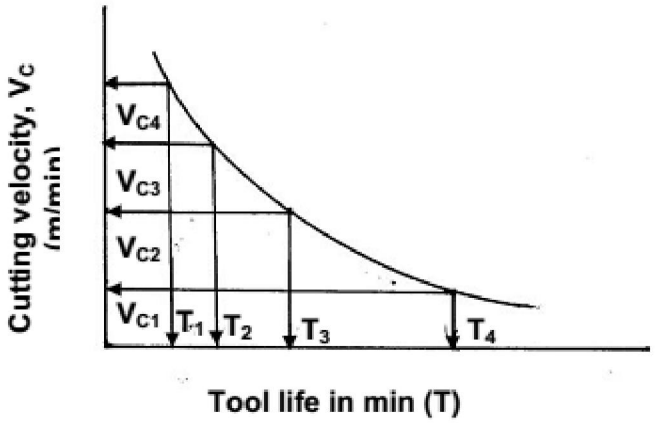

Fig. 4.9 Cutting velocity – tool life relationship

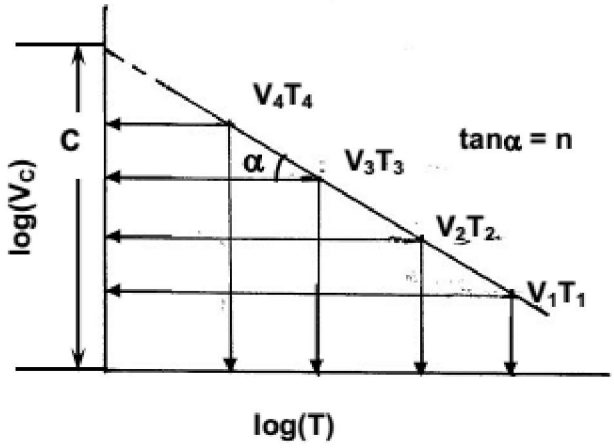

Fig. 4.10 cutting velocity vs. tool life on a log-log scale

Economics of machining

Basic model to provide the average unit can be to produce a given work piece configuration at the sum of four costs.

1. Machining cost
2. Tool cost
3. Tool changing cost
4. Handling cost

Assumptions

1. The work piece material is homogeneous.
2. Tool geometry is preselected .
3. The feed and depth of cut are preselected and constant .
4. Sufficient power is available to undertake the operation.
5. Cost per operating time is independent of actual cutting time.

Economic tool life : Gilbert's Model

Gilbert has evaluated tool life for

1. Minimum cost
2. Maximum production

$$\text{Cost per piece} = \frac{idle\ cost}{piece} + \frac{cutting\ cost}{piece} + \frac{tool\ changing\ cost}{piece} + \frac{tool\ regrinding\ cost}{piece}$$

Let k_1 = direct labour rate + over head rate, Rs/min

K_2= tool cost per grind ,Rs/tool

L= length of machining ,mm

D= diameter of machine part ,mm

V= cutting speed ,m/min

s= feed ,mm/rev

T_d= tool changing time.

- $\text{Idle cost/ piece} = K_1 * \left[\frac{idle\ time}{piece}\right]$
- $\text{Cutting cost/ piece} = K_1 * \frac{(\pi * D * L)}{(1000 * S * V)}$
- $\text{Tool changing cost/piece} = K_1 * \frac{tool\ failure}{piece} * T_d = K_1 * \left[\frac{\pi * D * L * V^{\left(\frac{1}{n}-1\right)}}{1000 * S * C^{\frac{1}{n}}}\right] * T_d$

- Total grinding cost per piece $= K_2 * \frac{tool\ failure}{piece} = K_2 * \left[\frac{\pi * D * L * V^{\left(\frac{1}{n}-1\right)}}{1000 * s * C^{\frac{1}{n}}}\right]$

- $cost/piece = K_1 * (idle\ time) + K_1 * \left[\frac{\pi * D * L * V^{\left(\frac{1}{n}-1\right)}}{1000 * s * C^{\frac{1}{n}}}\right] * T_d + K_2 * \left[\frac{\pi * D * L * V^{\left(\frac{1}{n}-1\right)}}{1000 * s * C^{\frac{1}{n}}}\right]$

For optimum cost per piece differentiating the above equation & equation to zero

$$\frac{d}{dv}(cost/piece) = 0$$

$$V_{opt} = C * \left(\frac{n}{1-n}\right)^n * \left[\frac{K_1}{K_1 * t_d + K_2}\right]^n$$

$$\text{Tool life for minimum cost} = \mathrm{T_{opt}} = \left[\frac{1}{\mathrm{n}} - 1\right] * \left[\frac{K_1 * t_d + K_2}{K_1}\right]$$

Optimal cutting speed for maximum production

If the cost in the basic model for machining are not considered an alternative model can be build for yielding the time required to produce a wrong piece

Let t_c = m/c time

T = tool life

t=tool changing time

t_l= handling time(idle time)

So unit time per work piece is

$$t_p = t_c + t_d * \frac{t_c}{T} + t_c \qquad [1]$$

Production rate (Q)=$\frac{1}{\mathrm{t_p}}$

The minimum unit time will result in maximum production rate. So differentiating equation [1] w.r.t cutting speed & equating to zero

$$V'_{opt} = \frac{C}{\left[\left[\frac{1}{\mathrm{n}}-1\right] * t_d\right]^n}$$

Tool life per maximum production rate

$$T'_{opt} = \left[\frac{1}{\mathrm{n}} - 1\right] * t_d$$